Environmental Science Advances

PAPER

View Article Online
View Journal | View Issue

Cite this: *Environ. Sci.: Adv.*, 2026, **5**, 169

Utilizing PMF and Monte Carlo-based models to evaluate toxic metal enrichment pathways, sources, and public health risks in an unplanned urbanized dumpsite soil

Hrithik Nath, [ab] Sajal Kumar Adhikary, [a] Srabanti Roy,[d] Sunjida Akhter,[e] Ummey Hafsa Bithi,[f] Mohammed Abdus Salam,[g] Abu Reza Md. Towfiqul Islam [h] and Md. Abu Bakar Siddique *[c]

Improper waste management in municipal dumpsites raises health concerns due to toxic elements (TEs). This study evaluates the enrichment, sources, and public health risks of TE contamination in an urban dumpsite in a southeastern city of Bangladesh. Nine TEs were determined spectrophotometrically from 175 representative soil samples of 35 sites. Pollution indices, the Positive Matrix Factorization (PMF) model, and Monte-Carlo Simulation (MCS) were employed in assessing contamination levels, apportion sources, and associated public health risks. The results revealed significant topsoil contamination, with Cd contributing 91% to the overall ecological risk. Three distinct sources contributing to TE contamination were identified: industrial sources (F_1, 15.78%, dominated by Cd), geogenic origins (F_2, 40.93%, characterized by Fe, Co, Mn, and Ni), and mixed residential/commercial/traffic sources (F_3, 43.30%, with high loadings of Cu, Zn, Pb, and Cr). Health risk assessment (HRA) revealed that children faced 4.61 times higher non-carcinogenic risk (NCR) and 2.53 times higher carcinogenic risk (CR) compared to adults. NCRs were primarily driven by Fe and Mn, while Ni, Cd, and Cr were the main contributors to CRs, exceeding acceptable limits. Using the PMF-HRA method, F_2 was identified as a significant source of both NCR (79.27% in children and 88.69% in adults) and CR (66.18% in children and 61.63% in adults), with F_3 also posing significant risks, particularly for children. These results highlight the urgent need for comprehensive waste management reforms and targeted remediation strategies at the studied dumpsite to mitigate TE contamination, safeguard public health, and protect the surrounding environment, particularly for vulnerable populations and critical infrastructure in the region.

Received 19th May 2025
Accepted 20th October 2025

DOI: 10.1039/d5va00141b

rsc.li/esadvances

Environmental significance

Rapid and unplanned urbanization results in the excessive dumping of municipal waste in the studied dumpsite comprising non-biodegradable hazardous metals. The residents have experienced several health and environmental consequences due to improper waste management in the region. The ecosystems in the region are at high risk. The agricultural lands are contaminated with heavy metals like Cd affecting the food chain. Due to its proximity to residential areas, waste incineration impacts human health. Children are at higher risk than adults with ingestion and inhalation exposure pathways. The Monte Carlo method revealed a 100% probability of total cancer risk for all age groups.

[a]*Department of Civil Engineering, Khulna University of Engineering & Technology (KUET), Khulna, 9203, Bangladesh*

[b]*Department of Civil Engineering, University of Creative Technology Chittagong (UCTC), Chattogram, 4212, Bangladesh*

[c]*Institute of National Analytical Research and Service (INARS), Bangladesh Council of Scientific and Industrial Research (BCSIR), Dhanmondi, Dhaka, 1205, Bangladesh. E-mail: sagor.bcsir@gmail.com*

[d]*Department of Public Health, University of Creative Technology Chittagong (UCTC), Chattogram, 4212, Bangladesh*

[e]*Department of Chemistry, Hajee Mohammad Danesh Science and Technology University, Dinajpur 5200, Bangladesh*

[f]*Institute of Food Science and Technology (IFST), Bangladesh Council of Scientific and Industrial Research (BCSIR), Dhanmondi, Dhaka, 1205, Bangladesh*

[g]*Department of Environmental Science and Disaster Management (ESDM), Noakhali Science and Technology University (NSTU), Noakhali 3814, Bangladesh*

[h]*Department of Disaster Management, Begum Rokeya University, Rangpur 5400, Bangladesh*

1. Introduction

Rapid urbanization and industrial expansion in developing countries, particularly in densely populated areas with limited infrastructure, have created significant waste management challenges, threatening environmental sustainability and public health.[1,2] As cities grow, the volume of waste often exceeds the capacity of existing systems, leading to uncontrolled waste burning, a widespread and hazardous practice in developing countries like Bangladesh.[3,4] This practice releases toxic elements (TEs) that accumulate in soil and water, causing long-term ecological damage and adverse health outcomes.[5,6] The lack of adequate waste management infrastructure and regulatory enforcement exacerbates the issue, highlighting the urgent need to understand the scale of contamination and develop effective strategies to mitigate its impacts.[7,8]

TEs released from waste burning at dumpsites pose serious environmental and health risks due to their persistence and non-degradability.[9,10] Incineration and uncontrolled open burning of municipal solid waste emit TEs (*e.g.*, Pb, Cr, Cd, Ni, *etc.*), which accumulate in soil and air, leading to prolonged contamination.[6,11] These TEs do not break down naturally,[12] allowing them to persist for decades and continuously expose populations to harmful effects.[13] Prolonged exposure to these TEs through inhalation, ingestion, and dermal contact significantly increases the risk of respiratory diseases, neurological disorders, kidney damage, cardiovascular issues, and various cancers, with children and pregnant women being particularly vulnerable due to their heightened sensitivity.[14–16] Furthermore, TE pollution disrupts soil nutrient balance, reduces biodiversity, and impairs ecosystem functions, posing long-term ecological threats.[17,18] To effectively tackle these persistent environmental and public health challenges, it is crucial to primarily conduct comprehensive assessments of exposure levels to TEs, identify the possible sources of these elements, and evaluate the associated health risks.

Source apportionment is a vital tool for identifying the origins of pollutants, offering a scientific foundation for targeted emission reduction strategies.[19,20] Among the various quantitative techniques available, receptor models such as the Chemical Mass Balance (CMB) model, UNMIX model, Principal Component Analysis/Absolute Principal Component Score (PCA/APCS) model, and Positive Matrix Factorization (PMF) model are commonly used. In recent years, the PMF model has gained widespread recognition due to its ability to quantify the contributions of potential pollution sources for each data point, effectively handle uncertainties, and incorporate non-negative constraints, ensuring practical and interpretable results.[21,22] Its reliability and accuracy have been validated in numerous studies, where it has been successfully applied to identify and quantify the sources of TEs in soil, establishing it as a robust analytical tool.[23,24] Furthermore, integrating PMF with other analytical techniques has proven effective in improving overall source apportionment as this approach improves the differentiation between natural and anthropogenic sources, refines contribution estimates, and strengthens overall data interpretation. For instance, Du *et al.* (2025)[25] combined PMF with correlation analysis and PCA to distinguish between natural and anthropogenic sources of heavy metals. Similarly, El Fadili *et al.* (2024)[26] integrated PMF with PCA and enrichment factor (EF) analysis to evaluate contamination sources and their relative impacts, highlighting the advantages of using complementary methods for more accurate and reliable apportionment results.

Assessing the health risks associated with exposure to TEs from the soils of dumpsites requires a comprehensive and realistic approach that accounts for variability and uncertainty in exposure parameters. Many recent research studies have relied on conventional models with specific deterministic parameters for health risk assessment (HRA).[27–29] Given the uncertainties in concentrations and individual differences, using a point estimation approach with fixed parameters to precisely determine the most hazardous TE for individuals is challenging, as it could lead to either underestimating or overestimating the actual risk.[30] Overestimated HRA may lead to unnecessary resource expenditure on remediation efforts, while underestimated HRA can result in serious health repercussions for residents near the dumpsites.[31] The Monte Carlo simulation (MCS) method, a well-established probabilistic health risk assessment (PHRA) tool, offers precise risk estimation by accounting for the possibility of TE exposure exceeding guideline thresholds while using repeated sampling within probability distributions to reduce uncertainty and identifying key elements for controlling potential risks.[31,32] By integrating source apportionment findings with PHRA through the PMF-HRA model, specific pollution sources can be directly linked to their associated health risks, enabling the development of targeted and scientifically informed mitigation strategies.[33,34] This integrated approach is critical for addressing the health and environmental challenges posed by TE contamination from waste burning, ensuring the protection of public health and the preservation of ecological systems.

Feni, a rapidly urbanizing city in southeastern Bangladesh with a population of approximately 234 350 and an annual growth rate of 3.5%,[35] faces significant waste management challenges, generating 70–80 tons of waste daily.[36] This has led to improper waste disposal at the city's largest dumpsite, Dewanganj, where waste has been openly dumped and burned for over 25 years (Fig. 1a).[37] As the primary waste repository for Feni Municipality, the dumpsite receives a diverse mix of residential, commercial, healthcare, and industrial waste, including food scraps, plastics, medical waste, and industrial by-products.[37] Residents have consistently raised concerns about health and environmental hazards, such as foul odors and pest infestations, yet local authorities have struggled to implement effective solutions.[36–38] Despite the critical need to assess TE contamination and its associated public health and ecological risks, no study has investigated the long-term pollution and health impacts at Dewanganj, particularly given its proximity to densely populated areas and decades of uncontrolled waste accumulation. Therefore, this study was designed to present the first comprehensive assessment of TE contamination at this long-polluted dumpsite, addressing

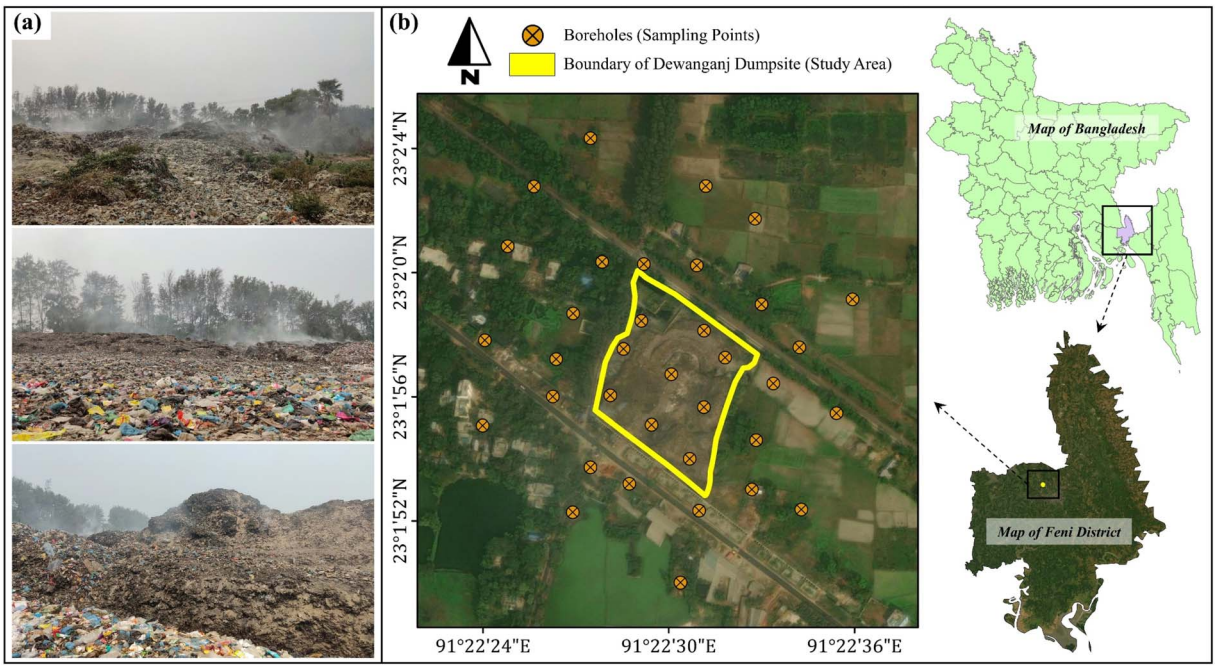

Fig. 1 (a) Uncontrolled waste disposal and open burning activities at Dewanganj dumpsite, Feni, and (b) locations of sampling points within the study area at the Dewanganj dumpsite.

a critical research gap through three primary objectives: (1) evaluating the spatial distribution and contamination levels of TEs in surface soil samples using multiple pollution assessment indices; (2) identifying potential sources of TE contamination through clustering, correlation, and PMF models; and (3) assessing ecological and human health risks associated with TE exposure using both deterministic and MCS models. The findings of this study are expected to provide critical insights for evidence-based policy interventions and the development of sustainable waste management strategies in Feni.

2. Materials and methods

2.1. Study site and situation of waste management

The study site, the Dewanganj dumpsite, spans approximately 4.28 acres and is situated in the 8th Ward of Feni Municipality (23°01′54″N, 91°22′28″E) in southeastern Bangladesh (Fig. 1b). Feni Municipality, established in 1958, is one of the oldest and fastest-growing district-level municipalities in the Chittagong Division, located 161 km south of the country's capital. The dumpsite is strategically positioned, bordered by the old Dhaka-Chittagong Highway to the south, the main railway line to the north, agricultural fields to the east and north, and residential and commercial zones to the west, southwest, and south. As the primary waste repository for all 18 wards of Feni Municipality, the site receives a heterogeneous mix of waste from residential, commercial, healthcare, industrial, and agricultural sources.[37] This includes biodegradable materials such as food scraps and vegetable peels from households and restaurants, plastic waste like packaging materials and single-use plastics from commercial establishments, medical waste from nearby healthcare facilities, industrial by-products such as metal scraps and chemical residues, and farming or agricultural wastes, including crop residues and organic matter from surrounding farmlands.

The waste management process at the dumpsite follows a diurnal cycle, with waste collected nocturnally from the city and deposited at the site in the morning. However, the site operates without regulatory controls or environmental safeguards. Of particular concern is the long-standing practice of indiscriminate waste dumping and frequent open burning, which has persisted for over 25 years without protective measures. These practices release malodorous emissions and hazardous residues into the environment, while the atmospheric dispersion of fly ash, due to the lack of containment infrastructure, extends contamination beyond the site boundaries. The environmental and health impacts are significant, with residents reporting respiratory ailments and other health issues exacerbated by waste combustion. The impact radius extends up to 4–5 km during the dry season, while the rainy season intensifies odor-related problems. Morning incineration activities particularly affect vulnerable groups, including school-going children and the working class. Given its proximity to residential areas, agricultural lands, and critical transportation infrastructure, the Dewanganj dumpsite represents a complex environmental and public health challenge. This makes it a critical focus for scientific research, offering an opportunity to elucidate the multifaceted impacts of inadequate waste management and inform the development of effective remediation strategies.

2.2. Soil sample collection, processing, and acid digestion

Soil samples were gathered in December 2023, during the dry season, to obtain maximum TE concentrations, as previous

studies have shown that pollution levels are reduced during the wet season due to heavy rainfall leading to infiltration and surface runoff.[39] Based on a reconnaissance survey, a total of 175 soil samples were collected from 35 selected representative sampling locations, with 9 situated within the dumping site and 26 from the nearby regions, and a GPS device was used to note the positions of these points. At every sampling location, five samples ($n = 5 \times 35 = 175$) were gathered from a 1 m × 1 m area (depth 0–10 cm), combined thoroughly to make a total of 35 representative composite samples, and then placed in clean zip-lock plastic bags immediately to protect them from weathering and contamination.[40]

Upon arrival at the laboratory, the samples were air-dried naturally for seven days at room temperature, followed by oven drying at 110 °C for 24 hours. Non-sediment materials were removed, and the samples were homogenized, crushed, and sieved through a 2 mm nylon mesh. The samples were then stored in airtight zip-lock polythene bags at 4 °C until analysis.[41] For acid digestion, about 10 g of the homogenized soil samples were mixed with a mixture of concentrated nitric acid and perchloric acid (in a 2 : 1 ratio) in pre-cleaned 250 mL glass beakers and heated on a hot plate at 100–110 °C under a fume hood until the residual organic materials decomposed and evaporated. The process of acid mixture addition and subsequent heating was repeated until a transparent solution was obtained. The samples were then filtered using Whatman-1 qualitative filter paper in beakers, and the filtered solution was re-heated with the addition of 2 mL concentrated nitric acid, and transferred to 100 mL calibrated volumetric flasks. The sample beakers were rinsed with deionized water several times to ensure the complete transfer of sample solutions, and the final volume of the samples was made up to 100 mL in the flasks (up to the mark) and stored at 4 °C until elemental analysis.[42,43] A sample blank was also prepared similarly to avoid contamination.

2.3. Spectrophotometric analysis of samples and quality control protocols

An atomic absorption spectrophotometer (AAS, Model: AA240FS, Varian, Australia) was used for the analysis of 9 TEs *viz.*, Cd, Co, Cr, Cu, Fe, Mn, Ni, Pb, and Zn in the digested soil samples due to their environmental persistence, potential toxicity, and common association with municipal and industrial waste.[44,45] These elements were selected based on their frequent occurrence in previous studies on dumpsite contamination and their known ecological and human health risks.[46]

During instrumental analysis, the calibration curves for each element were first constructed by measuring the working standard solutions of individual metals of different concentrations prepared from the stock solutions (1000 mg L^{-1}) of the certified reference materials (CRMs, Fluka Analytical, Sigma-Aldrich, Germany) diluted with deionized water. The concentration of the TEs in the soil sample solutions was determined with respect to their respective calibration curves through the absorbance measurement. To account for metals, present at elevated concentrations, the soil samples were diluted and measured when necessary, thus ensuring the absorption of the metals in the samples within the respective calibration curve range. While testing, the reagent blank sample was measured after every five soil samples, and standard and spike samples were determined after ten soil samples to ensure consistent measurement reliability. The analysis of TEs in this study was carried out at the INARS, BCSIR, Dhaka, Bangladesh. This laboratory operates according to ISO/IEC 17025:2017 accreditation for testing and calibration laboratories.

Good analytical laboratory practices were ensured while preparing and analyzing the samples in the laboratory with calibrated instruments and skilled analysts. To prevent any potential contamination, strict precautions were maintained during sample collection, transportation, storage, and laboratory analysis. Throughout the entire process, strict quality control measures were followed including the use of high-quality deionized water (conductivity <0.5 μS cm^{-1}), analytical-grade acids, a calibrated digital electrical balance with 4 significant figures in weighing, and calibrated glassware. Instrumental data calculations were based on the average of three consecutive measurements of the same sample, with a relative standard deviation (RSD) under 5%. The reliability of the analytical method was reinforced through spike recovery tests, which ranged from 90 to 110% (±10% acceptable error) of the expected values. The precision and accuracy of the analytical methods were tested with the CRMs as traceable to the NIST, USA. Further details of the analytical techniques with quality assurance and quality control schemes can be found in our previous studies.[42,43,47]

2.4. Evaluation of TE contamination in dumpsite soil

To comprehensively assess TE contamination in Dewanganj dumpsite soil (DSS), six key indicators were employed: the Coefficient of Variation (CV), geoaccumulation index (I_{geo}), Enrichment Factor (EF), Contamination Factor (CF), modified degree of contamination (mC_d), Pollution Load Index (PLI), and Nemerow Integrated Pollution Index (NIPI). These indicators provide different viewpoints on soil pollution, enabling a comprehensive assessment of both specific metal concentrations and the overall degree of contamination at dumpsites. The classification criteria for these indices are presented in SI Table S1. The CV is a key indicator of TE pollution patterns with higher CV values indicating greater heterogeneity, often suggesting influences of external factors, while lower values suggest a homogeneous distribution, generally indicative of geogenic origins.[24,48]

The CF, I_{geo}, and EF were applied in a complementary manner to evaluate element-specific contamination levels and potential anthropogenic influences, collectively strengthening the robustness of contamination assessment by capturing magnitude, severity, and source characteristics.[42,49,50] Although all three indices rely on background concentrations, each provides a distinct perspective. The CF offers a straightforward, linear measure of contamination magnitude relative to baseline values,[51] while I_{geo} employs a logarithmic scaling with a correction factor to minimize natural geochemical variability, thereby

classifying contamination into standardized severity categories.[52] The EF, by normalizing target element concentrations against a conservative reference element, helps to differentiate natural lithogenic contributions from anthropogenic enrichment.[53] Numerous studies have indicated that EF values below 2 are typically associated with natural metal sources, while values exceeding 2 suggest anthropogenic pollution.[16,54] Fe has been extensively used in soil contamination studies as the reference element for EF calculation due to its association with fine solid surfaces, similar geochemistry to many trace metals, and uniform natural concentration, which led to the selection of Fe in this study to ensure the reliable distinctions between natural and anthropogenic contributions to toxic element contamination.[55–57] The mC_d, PLI, and NIPI offer broader perspectives on overall site contamination, considering the combined effects of multiple pollutants.[58–60] By employing this varied range of metrics, it was possible to gain a detailed insight into the patterns and extent of TE pollution in DSS.[61] This approach facilitates more accurate environmental risk evaluations and aids in creating focused remediation plans for contaminated areas.

2.5. TE source analysis with clustering, correlation, and PMF models

Source apportionment, the process of determining and quantifying the possible origins of contaminants, is crucial in waste dumpsites to determine the primary contributors to TE contamination.[62,63] This knowledge facilitates the formulation of tailored intervention strategies and informs policy determinations aimed at lessening the detrimental impacts on human wellbeing and natural environments.[64,65] Multivariate statistical techniques renowned for their ability to analyze complex datasets, such as Hierarchical Cluster Analysis (HCA), Pearson's Correlation Matrix (PCM), and Positive Matrix Factorization (PMF) model, were utilized to unravel the most likely origins of TE contamination within the dumping site. HCA can effectively help in identifying possible sources of TEs by grouping samples with similar concentrations.[66] By examining a resulting dendrogram, inferences on potential contamination sources can be made based on the clustering patterns.[67] This analytical approach offers a visual and structured framework for elucidating the distribution patterns and source attribution of TEs. Extant scholarly literature suggests that correlation analysis can offer valuable insights into the potential co-existence and interrelationships within numerous TE pollutants existing in soil samples collected from waste disposal sites.[68,69] Consequently, PCM was employed to determine if the metal concentrations in the sediments were interrelated under the determined factors of PMF.[70]

However, it is well-documented that while correlation analysis can provide an initial indication of contamination sources, it does not inherently imply a causal relationship.[71,72] Therefore, the PMF model was employed to achieve a more comprehensive understanding of how many different sources contributed to the studied TEs in the DSS. This USEPA-endorsed model[73] employs a multivariate factor analysis technique that breaks down the original dataset into two distinct matrices: a factor contribution matrix (G_{ik}) and a factor distribution matrix (F_{kj}), along with a residual error matrix (E_{ij}), while maintaining a non-negative constraint.[74,75] By incorporating details on metal concentrations in samples and the associated levels of uncertainty, the PMF model produces outputs that determine the TE contamination sources. Assuming the concentration of TEs is a linear combination of contributions from various sources, the PMF model determines the relative contributions of these sources by analyzing the chemical mass balance expressions.[75,76] The foundational concentration data matrix can be derived using eqn (1). In this matrix, X_{ij} denotes the concentration of the j-th TE at the i-th sampling location, G_{ik} represents the influence of the k-th source on the i-th sample, and F_{kj} indicates the concentration of the j-th element from the k-th source.

$$X_{ij} = \sum_{k=1}^{p} G_{ik} F_{kj} + E_{ij} \quad (1)$$

The matrix of residual errors E_{ij} (eqn (2)) is derived by optimizing the objective function Q. In this case, U_{ij} signifies the uncertainty related to the concentration of the j-th TE in the i-th specimen. This value is derived from the species-targeted method detection limit (MDL), the actual concentration measured, and the associated error fraction. The model's goodness of fit is assessed using Q and the optimal number of factors was identified by achieving a stable and minimal Q value.[77]

$$Q = \sum_{i=1}^{n} \sum_{j=1}^{m} \left[\frac{E_{ij}}{U_{ij}}\right]^2 \quad (2)$$

The degree of uncertainty can be determined utilizing eqn (3), in which C denotes the pollutant concentration and σ represents the percentage of measurement uncertainty.[75,78]

$$U_{ij} = \begin{cases} 0.83 \times \mathrm{MDL}, & \text{when } C \le \mathrm{MDL} \\ \sqrt{[\sigma \times C]^2 + [0.5 \times \mathrm{MDL}]^2}, & \text{when } C > \mathrm{MDL} \end{cases} \quad (3)$$

PMF graphs, illustrating both the concentrations and percentages of TEs, provide essential insights into source apportionment.[79] An r^2 value greater than 0.6 is generally considered indicative of a strong predictive model. When the r^2 value falls below this threshold, the associated TEs are classified as "weak", signifying a higher uncertainty level in the model's result.[16,80] The presence of outliers can notably skew the analytical outcomes of the PMF model.[77] To address this issue, it is crucial to identify and remove outliers using methods such as histograms or interquartile range box plots before applying the model.[81] In this research, PMF analysis was executed following the systematic removal of outliers from the dataset.

2.6. Ecological risk assessment in the dumpsite area

The ecological risk assessment utilizes the approach initially proposed by Hakanson (1980)[50] and later revised by Xu *et al.*

(2008).[82] This method evaluates both individual (E_i) and combined ecological risks (ERI) posed by TEs in the dumpsite (eqn (4)). The ERI incorporates toxic-response factors for each TE, endorsing a nuanced ecological sensitivity estimation against different contaminants.[83] Through this approach, it is possible to deliver an extensive view of the total ecological risk arising from TE contamination in the study area.[39] The assessment categorizes both individual metal risks and combined risks into different levels of ecological concern, ranging from low to very high risk.[6,49,84] This classification system enables a clear interpretation of the potential ecological impacts and aids in prioritizing remediation efforts. By employing these ecological risk assessment methods, it is possible to gain a valuable understanding of the potential long-term environmental consequences of TE contamination at waste disposal sites.[85,86] This information can be crucial for developing effective environmental management strategies and guiding decisions on on-site remediation and ecosystem protection.[87,88]

$$\mathrm{ERI} = \sum E_i = \sum \left[\frac{T_i \times C_i}{B_i}\right] \quad (4)$$

The calculated E_i and ERI values were classified into risk categories to interpret the severity of potential ecological repercussions.[6,49,84] The detailed evaluation categories for the individual and total ecological risks are tabulated in SI Table S1.

2.7. Calculation-based health risk assessment

The human health risk assessment (HRA) follows a USEPA-endorsed model for evaluating both non-carcinogenic risk (NCR) and carcinogenic risk (CR).[89,90] This approach considers three primary exposure pathways: direct soil ingestion, inhalation of airborne particulates, and dermal absorption. Average Daily Doses (ADDs) are computed for various pathways and population groups, including landfill workers and nearby residents, using eqn (5)–(7), with parameters detailed in SI Table S2.[91] NCR is evaluated using the hazard quotient (HQ) approach (eqn (8)), which compares exposure levels to reference doses (RfD) for each TE and exposure route,[92] as tabulated in Table S3. The hazard index (HI) is calculated using eqn (9) to assess cumulative NCRs from multiple exposure pathways and TEs.[16] TEs identified as carcinogenic, such as As, Cd, Pb, Ni, and Cr, are evaluated for CR.[93] The cancer risk (CRI) and incremental lifetime cancer risk (ILCR) are calculated using pre-defined standard cancer slope factors (CSFs) (Table S3) for each exposure pathway using eqn (10) and (11), respectively.[94,95] Eventually, total carcinogenic risk (TCR) is calculated using eqn (12) which indicates the ultimate CR at the site. Using these risk assessment methods, it is possible to gain crucial insights into potential health impacts on different population groups, enabling informed decision-making for safeguarding public health and managing sites effectively.[96,97]

$$\mathrm{ADD_{ing}[mg\ per\ kg\ per\ day]} = \mathrm{TEC} \times \frac{\mathrm{IGR} \times \mathrm{EF} \times \mathrm{ED}}{\mathrm{ABW} \times \mathrm{AT}} \times 10^{-6} \quad (5)$$

$$\mathrm{ADD_{inh}[mg\ per\ kg\ per\ day]} = \mathrm{TEC} \times \frac{\mathrm{INR} \times \mathrm{EF} \times \mathrm{ED}}{\mathrm{ABW} \times \mathrm{AT} \times \mathrm{PEF}} \quad (6)$$

$$\mathrm{ADD_{der}[mg\ per\ kg\ per\ day]} = \mathrm{TEC} \times \frac{\mathrm{ESA} \times \mathrm{SAF} \times \mathrm{ABS} \times \mathrm{EF} \times \mathrm{ED}}{\mathrm{ABW} \times \mathrm{AT}} \times 10^{-6} \quad (7)$$

$$\mathrm{HQ_{ing/der/inh}} = \frac{\mathrm{ADD_{ing/der/inh}}}{\mathrm{RfD_{ing/der/inh}}} \quad (8)$$

$$\mathrm{HI} = \mathrm{HQ_{ing}} + \mathrm{HQ_{der}} + \mathrm{HQ_{inh}} \quad (9)$$

$$\mathrm{CRI_{ing/der/inh}} = \mathrm{ADD_{ing/der/inh}} \times \mathrm{CSF_{ing/der/inh}} \quad (10)$$

$$\mathrm{ILCR} = \mathrm{CRI_{ing}} + \mathrm{CRI_{der}} + \mathrm{CRI_{inh}} \quad (11)$$

$$\mathrm{TCR} = \sum \mathrm{ILCR}_i \quad (12)$$

2.8. Monte Carlo simulation-based probabilistic health risk appraisal

The Monte Carlo simulation (MCS) approach was utilized to conduct a probabilistic risk assessment, which was specifically chosen to address the limitations of using deterministic parameters, which can lead to either overestimating or underestimating health risks.[98] This approach allows for a more comprehensive evaluation of health risks by considering the uncertainties in TE concentrations and the variability of key exposure factors. These factors include how often and for how long exposure occurs, the rates of soil ingestion and inhalation, the area of skin exposed, and the average weight of individuals. A lognormal distribution was employed to model the TE concentration data. For the exposure factors, the most suitable probability distributions were selected by referring to previous studies in the field (Table S2). In this methodology, statistical random variables were generated from point inputs, and numerous iterations of HQ, HI, ILCR, and TCR calculations were performed. Each iteration utilized different randomly generated inputs, producing a distribution of risk values rather than a single estimate. The study employed a large number of simulations, specifically ten thousand iterations, to enhance the reliability of the findings at a 95% confidence interval. Following this, a sensitivity analysis was conducted to determine how different input parameters affected the results for both HI and TCR. The findings from this analysis were integrated into risk assessment.[99] Additionally, recent advancements led to the creation of the PMF-HRA model, which integrates results from MCS-based HRA and PMF models.[33,100] This model quantifies the impact of different sources on overall health risks. To achieve this, the health risks linked to each TE were adjusted according to the contribution rates of the identified sources, allowing for the assessment of health risks attributed to various sources.

2.9. Data analysis and statistical methods

Various statistical analyses were performed using SPSS v26.0, including descriptive statistics, PCM, and HCA. EPA PMF v5.0 was utilized to implement the PMF model for source

apportionment of contaminants. Inverse distance weighted (IDW) interpolation was employed to map the spatial distribution of TEs within the dumpsite, aiding in source identification and corroborating PMF results.[88,101] MCS was conducted using Crystal Ball v11.1.3.0 software to enhance risk assessment accuracy. Initial data visualization was done in Microsoft Excel and Origin v9.0, with final refinements made in Microsoft PowerPoint. Fig. 2 presents a comprehensive overview of the study's methodological approach.

3. Results and discussion

3.1. Distribution and contamination of TEs in dumpsite soil

The analysis of nine TEs in soil samples from the landfill site revealed complex spatial distribution patterns and varying concentration levels (Fig. 3). Table 1 and 2 present the respective average concentrations, standard deviations, CVs, ranges, and contamination indices of the studied TEs. While some metals showed minimal contamination despite high concentrations, others exhibited moderate to severe contamination levels.

The abundance of the TEs in the soil samples was observed to follow the order of Fe > Mn > Zn > Cu > Pb > Cr > Ni > Co > Cd. Fe exhibited the highest average concentration (10 331.2 mg kg^{-1}) with a wide range (980.1–16 114.1 mg kg^{-1}). The spatial distribution map for Fe demonstrated relatively uniform contamination with higher concentrations in the central and northern zones. However, its I_{geo} of −2.78 and CF of 0.22 suggested minimal contamination relative to the background value. Mn and Zn followed with average concentrations of 370.2 mg kg^{-1} and 253.1 mg kg^{-1}, respectively. The geographic distribution of manganese revealed elevated levels in the north and central areas. Concentrations in these regions reached as high as 1357.7 mg kg^{-1}, substantially exceeding the established background level of 850.0 mg kg^{-1}. Despite this, its I_{geo} (−1.78) and CF (0.44) indicated low contamination. Zn showed elevated levels in the central and southeastern zones, with concentrations up to 669.5 mg kg^{-1}, significantly exceeding the background value of 95.0 mg kg^{-1}. This was reflected in its I_{geo} (0.83) and CF (2.66), indicating moderate contamination. Cu displayed a notable average concentration of 193.1 mg kg^{-1}, ranging from 7.30 to 639.0 mg kg^{-1}. Major hotspots were observed in the central and southeastern areas, significantly exceeding the background value of 45.0 mg kg^{-1}. This was corroborated by its I_{geo} (1.52) and CF (4.29), suggesting moderate to considerable contamination. Pb exhibited an average concentration of 51.53 mg kg^{-1}, ranging from 9.15 to 134.0 mg kg^{-1}. Its spatial map showed notable areas of high concentration in the southeast and central regions, with levels reaching as high as 134.0 mg kg^{-1}, significantly exceeding the typical baseline of 20.0 mg kg^{-1}. This elevated presence was corroborated by the I_{geo} of 0.78 and CF of 2.58, suggesting a moderate level of environmental pollution.

Cr demonstrated an average concentration of 29.08 mg kg^{-1}, ranging from 8.87 to 69.80 mg kg^{-1}. Its spatial map exhibited elevated levels predominantly in the southern and central zones. However, its I_{geo} (−2.21) and CF (0.32) suggested minimal contamination. Ni, Co, and Cd exhibited the lowest average concentrations. Ni (average 23.29 mg kg^{-1}) showed elevated levels in the central and southwestern parts, while Co displayed high concentration areas in the eastern and

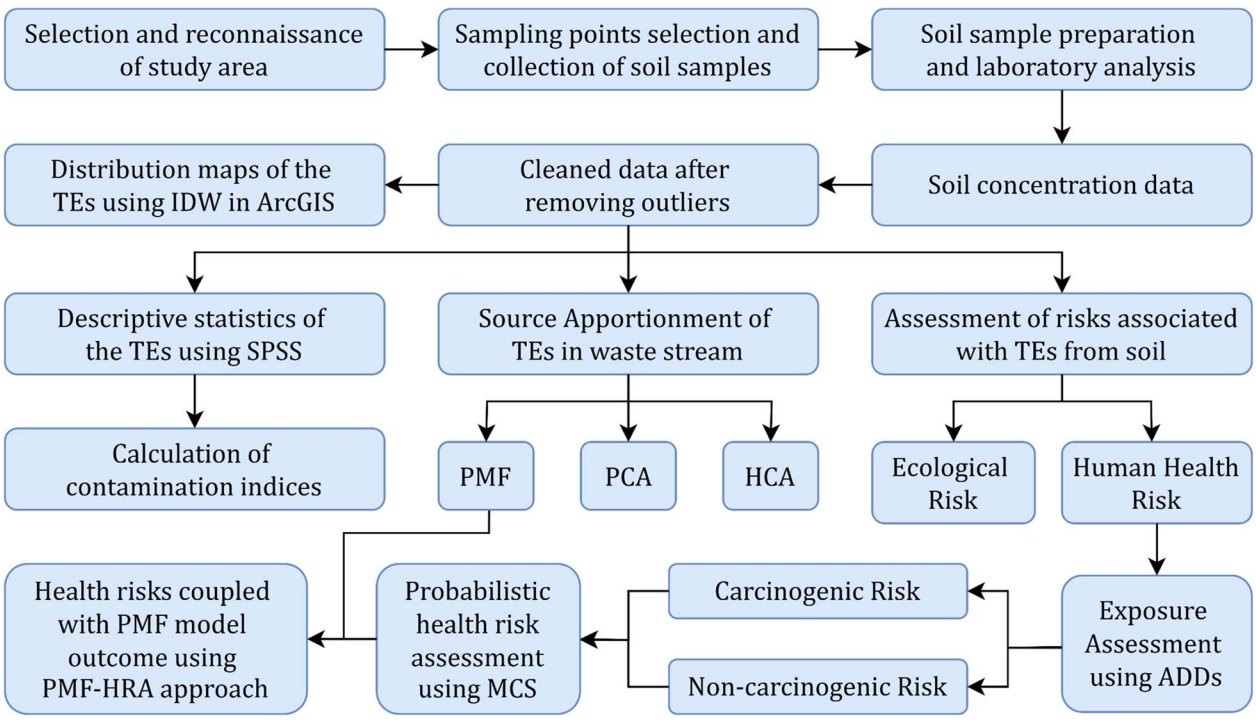

Fig. 2 Methodological flow chart of the current study.

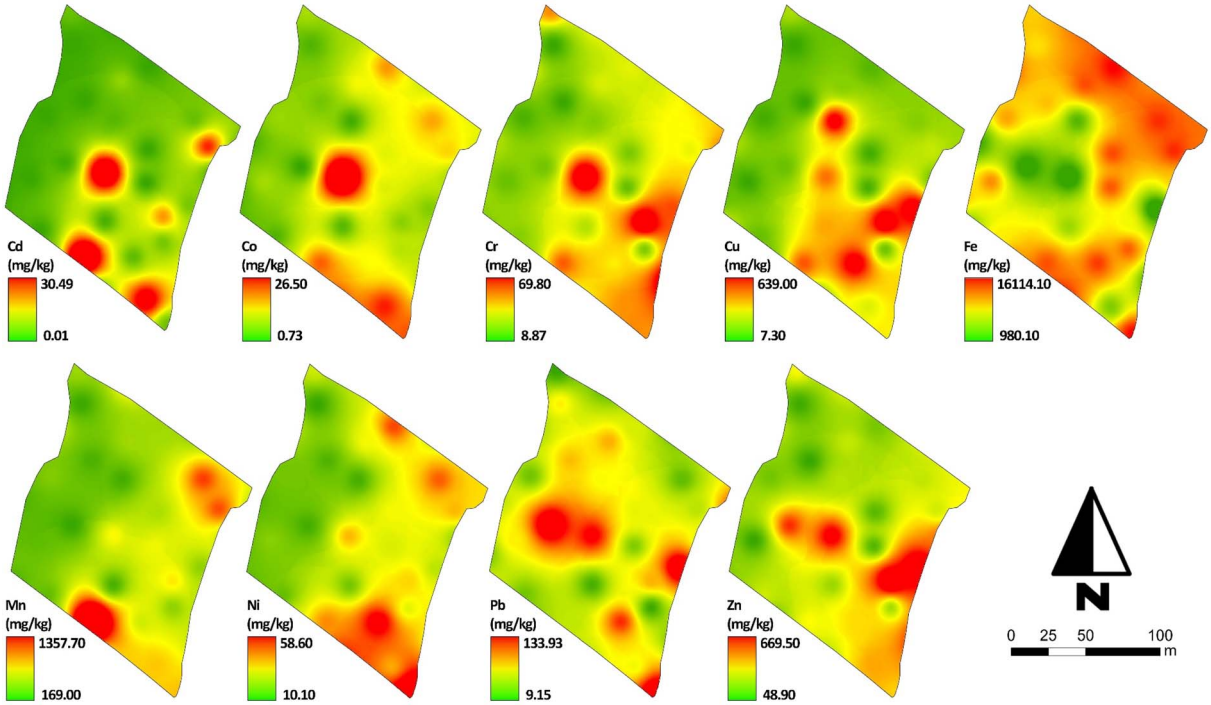

Fig. 3 Spatial distribution of TE concentrations within the dumpsite.

Table 1 Descriptive statistics and background values of TEs in the dumpsite soil[a]

TEs	Average	Range	SD	CV (%)	BGV
Cd	4.21	0.01–30.50	7.57	179.8%	0.30
Co	6.28	0.73–26.50	4.97	79.18%	19.0
Cr	29.08	8.87–69.80	15.31	52.64%	90.0
Cu	193.1	7.30–639.0	186.4	96.53%	45.0
Fe	10 331.2	980.1–16 114.1	4600.6	44.53%	47 200
Mn	370.2	169.0–1357.7	209.9	56.71%	850.0
Ni	23.29	10.10–58.60	10.32	44.31%	68.0
Pb	51.53	9.15–134.0	33.47	64.95%	20.0
Zn	253.1	48.90–669.5	156.7	61.90%	95.0

[a] Concentrations of all TEs are given in mg kg^{-1}, SD = Standard Deviation, CV = Coefficient of Variation, BGV = Background Value.

southwestern zones. Both Ni and Co had negative I_{geo} values and CF values less than 1, indicating minimal contamination. Notably, Cd, despite its low average concentration (4.21 mg kg^{-1}), showed several hotspots in the northeastern and central zones, with concentrations reaching up to 30.49 mg kg^{-1}, significantly above the background value of 0.30 mg kg^{-1}. This was reflected in its exceptionally high I_{geo} (3.23), EF (64.14), and CF (14.04), indicating severe contamination and anthropogenic impact. The combined application of CF, I_{geo}, and EF ensured a robust evaluation of soil contamination. While CF quantified contamination intensity, I_{geo} provided standardized severity classes, and EF distinguished anthropogenic from geogenic inputs. Together, they avoided misinterpretation and confirmed Cd as the dominant pollutant, with Cu, Pb, and Zn showing anthropogenic enrichment, and Fe, Mn, Ni, Co, and Cr remaining largely geogenic.

Overall site contamination was evaluated using multiple indices to ensure a comprehensive assessment. PLI yielded a value of 1.04, indicating slight contamination at the site. In contrast, NIPI produced a much higher value of 10.12, suggesting severe soil contamination. This discrepancy is attributable to the heightened sensitivity of NIPI to the most critical pollutant—in this case, Cd.[102] When all analyzed metals were considered collectively, an mC_d of 2.80 indicated moderate contamination. The results from EF analysis further supported these observations, with Cd exhibiting extreme enrichment (EF

Table 2 Contamination indices of TEs in the dumpsite soil[a]

	Element specific contamination indices			Overall site contamination indices		
TEs	I_{geo}	EF	CF	mC_d	PLI	NIPI
Cd	3.23	64.14	14.04	2.80	1.04	10.12
Co	−2.18	1.51	0.33			
Cr	−2.21	1.48	0.32			
Cu	1.52	19.60	4.29			
Fe	−2.78	1.00	0.22			
Mn	−1.78	1.99	0.44			
Ni	−2.13	1.56	0.34			
Pb	0.78	11.77	2.58			
Zn	0.83	12.17	2.66			

[a] I_{geo} = Geoaccumulation Index, EF = Enrichment Factor, CF = Contamination Factor, mC_d = Modified Degree of Contamination, PLI = Pollution Load Index, NIPI = Nemerow Integrated Pollution Index.

> 40), while Cu (19.60), Pb (11.77), and Zn (12.17) showed considerable enrichment, reflecting substantial anthropogenic inputs. The remaining trace elements displayed minimal enrichment, with EF values approximating 1.5, consistent with natural background contributions. The divergence between PLI (1.04) and NIPI (10.12) can be explained by their differing formulations: PLI, being a geometric mean, dampens variability across elements and underestimates the influence of a dominant pollutant, whereas NIPI, by emphasizing the maximum contamination factor, accentuates the role of the most critical element. In this case, Cd's disproportionately high contamination elevated the NIPI value, aligning with its dominance across CF, I_{geo}, EF, and ecological risk indices. Therefore, while PLI reflected slight overall contamination, NIPI more accurately captured the severity driven by Cd as the critical pollutant.

The heterogeneity of TE distribution using CV revealed moderate variation (10% ≤ CV < 100%) for most TEs, including Ni (44.31%), Fe (44.53%), Cr (52.64%), Mn (56.71%), Zn (61.90), Pb (64.95%), Co (79.18%), and Cu (96.53%). Cd exhibited a CV of 179.75%, indicating strong variation and significant spatial heterogeneity, reinforcing its severe contamination status.

3.2. Source apportionment of TEs in the dumpsite soil

The source apportionment results and factor contribution percentages from the PMF model for TEs in the samples analyzed are illustrated in SI Fig. S2 and 4a, respectively. The model output indicated that three factors were optimal for explaining the data variability. The residual values for most soil samples fell within the range of −3 to 3, suggesting a good model fit. The coefficient of determination (r^2) between predicted and observed values demonstrated strong correlations among the investigated metals, with Pb exhibiting the highest r^2 value of 0.998 and Mn showing the lowest. The PMF model results revealed significant variations in both concentrations and percentages of TEs across the three identified factors: Factor 1 (F_1) was dominated by Cd, Factor 2 (F_2) was characterized by Fe with notable contributions from Co, Mn, and Ni, and Factor 3 (F_3) showed high loadings of Cu, Zn, Pb, and Cr. HCA exhibited an identical trend of grouping, with three main clusters, depicted in the dendrogram (Fig. S1). The elements Co, Cr, Fe, Mn, and Ni were organized into one cluster, whereas Cu, Pb, and Zn were placed into a different cluster, and Cd was categorized into a separate cluster. PCM further clarified the relationships among the TEs, offering insights into the factor-based grouping patterns (Fig. 4b).

The TE pollution sources demonstrated complexity, as evidenced by the observed variations between metal concentrations and their percentage contributions. For instance, Cd, despite its low concentration, accounted for over 80% of F_1, whereas Fe, with a considerably higher concentration, constituted less than 5% (Fig. S2). This trend was consistently noted across various factors for other metals as well. The influence of a metal within a factor depends not only on its concentration but also on its relative proportion within that factor.[80] Although higher concentrations often result in larger contributions, the defining characteristic of a factor is typically its proportional representation. The PMF model, which provided graphical representations of both concentrations and percentages of TEs, has offered valuable insights into source apportionment. High positive correlations between key elements are generally regarded as indicators of simultaneous release and a shared origin for these metals.[68] That's why PCM was employed to evaluate if the TE concentrations in the DSS were correlated based on the factors determined by PMF.[70]

F_1 accounted for 15.78% of the total TE contribution and had a significant loading of Cd (82.26), posing a severe threat to the soil ecosystem, as confirmed by pollution indices (Table 2) and ecological indices (Table S4). Despite its low average concentration (4.21 mg kg^{-1}), Cd was 14 times higher than the background value (0.30 mg kg^{-1}), with the CF (14.04), I_{geo} (3.23), and EF (64.14) indicating extreme contamination. Its high CV (179.75%) reflected strong spatial variability, with hotspots in the northeastern and central zones, reaching 30.49 mg kg^{-1}. While other sources may contribute to the overall Cd pollution, the characteristics of F_1 and the local industrial profile strongly

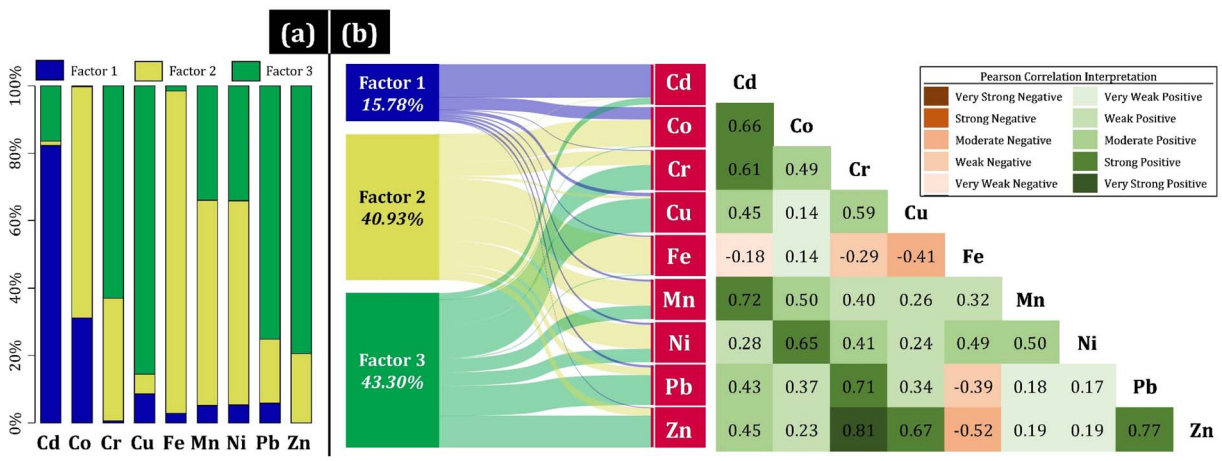

Fig. 4 Source apportionment of TEs in dumpsite soils: (a) factor profiles of TEs in soils of the dumpsite from the PMF model, and (b) correlation illustration between TEs using PCM combined with the PMF model.

support industrial waste incineration as the primary origin of the observed Cd pollution in the DSS. The presence of various industries, including textile, metal, paper and packaging, food, and manure production, provides strong evidence for this conclusion. Cd is widely used in industrial applications such as dyes in textiles,[103] slags from metal industries,[104] residues of fertilizer production,[105] and inks and pigments in paper and packaging,[106] all of which might have contributed to its accumulation in waste streams, with burning potentially releasing Cd into the DSS. Previous studies have also reported significant Cd enrichment near waste sites, reinforcing industrial activities as a key source of Cd pollution in the study area.[63,107]

F_2 was responsible for 40.93% of the total contribution and was characterized by significant loadings of Fe (95.57%), Co (68.54%), Mn (60.85%), and Ni (60.52%). PCA revealed moderate to strong correlations among these metals (*e.g.*, Ni–Co: $r = 0.65$; Fe–Ni: $r = 0.49$), suggesting a common source or similar environmental behavior, also supported by geochemical and ecological indices. Fe had the highest concentration among the TEs, but it was still significantly below the background value, indicating that Fe is not a major contaminant and presumably represents natural geological changes. However, its elevated concentrations in the northern study area suggest localized inputs, possibly from industrial activities. While Co, Mn, and Ni exhibited lower contamination indices, Co's high variability (79.18%) and concentration hotspots in the central and southwestern regions point to localized anthropogenic influence. Previous studies have identified these elements as major components of the Earth's crust as well, indicating that their presence is largely attributed to geological weathering.[24,108] Thus, although F_2 is largely geogenic, external factors might have contributed to localized pollution.

F_3, accounting for 43.30% of the total contribution, exhibited high loadings of Cu (85.60%), Zn (79.50%), Pb (75.17%), and Cr (63.02%), collectively posing a moderate risk to the DSS system. PCM analysis revealed strong correlations among these metals, including Cr–Zn ($r = 0.81$), Cu–Zn ($r = 0.67$), Cr–Pb ($r = 0.71$), and Pb–Zn ($r = 0.77$), suggesting a shared source. HCA grouped Cu, Zn, and Pb in one cluster, with Cr forming a separate group. High EF values for Cu (19.60), Cr (1.48), Pb (11.77), and Zn (12.17) indicated significant anthropogenic influence, with their average concentrations exceeding background levels by factors of 4.29, 1.48, 2.58, and 2.66, respectively, predominantly due to land-based waste processing. Wastes from households, local bazaars, shops and restaurants, regularly dumped at the Dewanganj dumpsite,[37] likely played a significant role in overall TE contamination and might have been major contributors to F_3 by introducing various contaminants. Organic waste, such as vegetable and fruit scraps, might have introduced Pb from contaminated soil and pesticide residues,[109] while fish and meat market waste might have contributed Pb through processing chemicals.[110] Discarded cans, plastics, papers, and broken glasses further introduce Pb and Cr due to manufacturing processes, inks, and coatings.[111–115] Electronic waste, particularly from discarded batteries, is a major source of Pb, Ni, and Cr.[116,117] Cu contamination, in particular, could have been attributed to electronics and electrical goods shops, which extensively use copper in wiring and components.[118] Furthermore, discarded clothing, garment, and fabric waste might have contributed Cu, Zn, Pb, and Cr due to the presence of metal-based dyes, fabric treatments, and synthetic coatings.[119–121] Additionally, waste from numerous local healthcare facilities and medical shops, including expired pharmaceuticals, blister packs, and discarded medical equipment, might have contributed Pb, Cu, and Zn due to the presence of metallic coatings, liquids, and certain drug formulations.[122–124]

While residential and market wastes appear to be the dominant contributors to F_3, the factor likely reflects a mix of anthropogenic sources. As a rapidly developing city, Feni generates substantial construction waste, which is disposed of in dumpsites, potentially contributing to F_3 through the release of Cu from electrical wiring and plumbing, Pb from lead-based paints, pipes, and ceramics, and Zn from galvanized steel and roofing materials.[125–128] Additionally, vehicular emissions from the highway in the southern part of the study area likely played a significant role in F_3. The strong correlation between Pb and Zn ($r = 0.77$) further supports this, as both metals are well-documented markers of traffic-related pollution.[129] Pb, historically used in gasoline as an anti-knocking agent, persists in soils despite its phase-out in many countries, while Zn is commonly released through tire wear and the corrosion of galvanized vehicle components.[130–132] Vehicle exhaust, brake wear, and the breakdown of lead–acid batteries also contribute to Pb deposition in adjacent soils, while Zn is predominantly introduced through tire abrasion and road runoff.[20,133]

Notably, Cr exhibited significant contributions across multiple factors, suggesting complex sources or environmental behaviors, but was grouped into F_3 due to its high correlation with Pb, Zn, and Cu. Although Cd was primarily associated with F_1, it also showed a strong association with Mn ($r = 0.72$) and moderate associations with Pb ($r = 0.43$) and Zn ($r = 0.45$). In PMF, the variations between concentration and percentage contribution in certain instances underscored the intricate nature of TE pollution sources. For example, although Cd had a low concentration, it represented over 80% of F_1, whereas Fe, despite its higher concentration, comprised less than 5% (Fig. 4a). This pattern was consistently observed across different factors for other metals as well. The impact of a metal on a factor is influenced not just by its concentration but also by its relative proportion within that factor. Therefore, while higher concentrations often lead to larger contributions, the defining feature of a factor is generally its proportional representation.

3.3. TE induced risk evaluation at the dumpsite

3.3.1. Ecological risk assessment. The ecological risk assessment of the TEs in the DSS revealed substantial concerns, as detailed in SI Table S4. The overall ecological risk (ERI) for the target TEs was 460.94, classifying the DSS as exhibiting a considerable ecological risk. Cd was identified as the primary contributor to ecological risk, comprising 91.36% of the ERI, with an E_i of 421.14, classifying it as posing a very high ecological risk at the studied site. Such dominance of Cd has been previously reported in other studies also, such as in

Enugu, Nigeria, where 91% of the ecological risk in a municipal DSS was attributed to Cd,[134] and in China, where Cd contributed 80% of the potential ecological risk in DSS impacted by industrialization and urbanization.[135] Another study revealed Cd to be posing the highest ecological risk among all the studied TEs and contributing more than 76% of the total ecological risk in an open solid waste dumpsite situated in central Thailand.[95] Conversely, a study in Uyo, Nigeria, revealed very low human health risk despite high ecological risk from Cd contamination in solid waste DSS.[39]

Cd is increasingly acknowledged as a significant environmental threat due to its harmful impacts on soil integrity, biological activities, plant physiology, and the health of humans and animals.[136] The EPA (Environmental Protection Agency) has identified this TE among the 126 priority pollutants, classifying it as a contaminant of concern.[137] It is highly bio-persistent, exhibiting toxicological effects and remaining in organisms for many years after consumption.[138] Soil is considered harmful when it contains more than 8 mg kg^{-1} of Cd,[139] and plants cultivated in soils that contain elevated Cd levels have been extensively documented to experience severe metabolic irregularities and oxidative stress.[140–144] Such stress disrupts crucial physiological processes, leading to morphological aberrations and compromised plant health.[145] These disruptions include impaired photosynthesis, nutrient imbalance, and inhibited growth, which collectively undermine plant productivity and biodiversity.[146] In addition, Cd-induced oxidative stress can cause cellular damage due to the development of reactive oxygen species (ROS), further exacerbating plant health deterioration.[147,148] These physiological and morphological effects on plant life can trigger a series of changes throughout the ecosystem, influencing soil quality, microbial activity, and the well-being of herbivores and other higher trophic levels that rely on these plants.[146,149,150] Therefore, the pronounced ecological risk posed by Cd necessitates urgent and robust remediation strategies to mitigate its adverse effects on the ecosystem, ensuring the preservation of biodiversity and ecosystem functionality. Conversely, the E_i values for Cu (21.45), Cr (0.64), Mn (0.44), Ni (1.71), Pb (12.88), and Zn (2.66) were relatively low, indicating low ecological risks at the studied dumpsite.

3.3.2. Exposure scenario of the TEs. A consistent hierarchy of exposure scenarios was observed across the three pathways, with the average daily dose (ADD) of TEs in DSSs indicating potential exposure risks for 2 age groups (children and adults) (Table S5). Fe was found to be the most predominant contaminant among the nine TEs examined in terms of exhibiting the highest ADD values across all exposure pathways. For children, the highest ADD values were observed for Fe, with an ADD_{ing} of 9.43×10^{-2} mg per kg per day, reflecting the significant amount of iron present in the soil. Following Fe, Mn had an ADD_{ing} of 3.38×10^{-3} mg per kg per day, and Zn presented an ADD_{ing} of 2.31×10^{-3} mg per kg per day. For adults, Fe also exhibited the highest ADD_{ing} value at 1.01×10^{-2} mg per kg per day, followed by Mn (3.62×10^{-4} mg per kg per day) and Zn (2.48×10^{-4} mg per kg per day). Comparatively, Cd, despite its high toxicity, presented lower ADD values for both children (3.85×10^{-5} mg per kg per day) and adults (4.12×10^{-6} mg per kg per day) due to its lower concentration in the soil. However, the toxicity of Cd necessitates attention even at these lower doses.

The ingestion pathway consistently showed higher exposure compared to dermal and inhalation pathways, emphasizing that soil ingestion is the primary exposure route for these populations. The ADD_{ing} values were typically found to exceed ADD_{inh} and ADD_{der} by several orders of magnitude. As an illustrative example, Pb in children exhibited ADD_{ing}, ADD_{inh}, and ADD_{der} values of 4.71×10^{-4}, 1.32×10^{-6}, and 1.79×10^{-8} mg per kg per day respectively. This pattern was consistently observed across all metals and age groups, with children demonstrating higher exposure levels compared to adults. In prior studies assessing health risks associated with TEs in soil, ingestion has been consistently recognized as the most dangerous exposure route for children, with dermal absorption and inhalation being secondary concerns.[95,151–154] Children often engage in outdoor play both at school and at home, along with crawling activities, which heighten their exposure to TEs *via* dermal contact.[155] Frequent hand-to-mouth actions further increase the risk of ingestion.[156,157] Given that children's average height is around 70–80 cm above ground, they are particularly susceptible to inhalation exposure, especially during dry seasons. However, inhalation exposure of re-suspended soil particles through the nose and mouth was found to be a bit less, ranging from 10^{-4} to 10^{-5} times lower than ingestion. On average, an adult breathes approximately 20 m^3 of air per day (0.014 m^3 min^{-1}), which may increase during vigorous activities.[158] This air can contain TEs from the dumpsite, entering the body through inhalation. Furthermore, adults might also be exposed to TEs due to insufficient hand washing before eating after daily activities.[159]

3.3.3. Probabilistic human health risk assessment. Table 3 presents the NCRs and CRs for children and adults from TE exposure, assessed *via* MCS across three exposure pathways. The NCR, measured by using HQ values, reflected the patterns of ADD. HI values for both groups followed the order Fe > Mn > Pb > Cr > Cu > Cd > Ni > Zn > Co. For children, HQ values were below 1 for most metals across all pathways, except for Fe in inhalation (HQ = 1.20) (Fig. 5). Inhalation was the primary risk contributor for both children (67.26% of total HI) and adults (78.36%), with Fe being the most significant contributor to adult HI (52.13%). Children showed a significant NCR (HI = 2.81), while adults had a lower risk (HI = 0.61). Notably, children's risk was substantially higher across all pathways: 9.34 times greater through ingestion, 2.33 times greater through dermal contact, and 1.54 times greater through inhalation (Table S6).

CR estimations were conducted only for Cd, Cr, Ni, and Pb due to their high toxicity levels and the availability of cancer slope factor (CSF) values.[16,160] The cumulative distribution functions (CDF) from MCS provided a nuanced understanding of risk occurrence and probabilities. The results revealed that the mean total cancer risk (TCR) for children was 4.99×10^{-5}, while for adults, it was 2.46×10^{-5}, both exceeding the lower limit of the acceptable CR range (Fig. 5k and S3). For adults, the 5th and 95th percentile TCR values, 1.19×10^{-5} and 4.34×10^{-5} respectively, were within the acceptable CR range.

Table 3 Probabilistic non-carcinogenic and carcinogenic health risks of each individual and combined TEs in the dumpsite soils for children and adults according to Monte Carlo simulations[a]

		Children			Adult		
Risk	TEs	Mean	SD	Interpretation	Mean	SD	Interpretation
HQ	Cd	4.32×10^{-2}	7.69×10^{-2}	No NCR	5.04×10^{-3}	8.50×10^{-3}	No NCR
	Co	3.03×10^{-3}	2.54×10^{-3}	No NCR	3.30×10^{-4}	2.81×10^{-4}	No NCR
	Cr	1.23×10^{-1}	7.07×10^{-2}	No NCR	1.76×10^{-2}	1.04×10^{-2}	No NCR
	Cu	4.69×10^{-2}	4.52×10^{-2}	No NCR	5.13×10^{-3}	5.09×10^{-3}	No NCR
	Fe	$1.45 \times 10^{+00}$	9.42×10^{-1}	Potential NCR	3.46×10^{-1}	1.50×10^{-1}	No NCR
	Mn	7.92×10^{-1}	5.87×10^{-1}	No NCR	1.92×10^{-1}	1.20×10^{-1}	No NCR
	Ni	1.15×10^{-2}	5.53×10^{-3}	No NCR	1.25×10^{-3}	6.23×10^{-4}	No NCR
	Pb	3.64×10^{-1}	2.40×10^{-1}	No NCR	3.96×10^{-2}	2.74×10^{-2}	No NCR
	Zn	8.34×10^{-3}	5.42×10^{-3}	No NCR	9.11×10^{-4}	6.09×10^{-4}	No NCR
HI	Total	2.81	1.32	Potential NCR	0.61	0.24	No NCR
Children/adult ratio	4.61						
ILCR	Cd	1.42×10^{-6}	2.87×10^{-6}	Acceptable CR	6.75×10^{-7}	1.23×10^{-6}	Negligible CR
	Cr	1.52×10^{-5}	1.12×10^{-5}	Acceptable CR	8.59×10^{-6}	5.11×10^{-6}	Acceptable CR
	Ni	3.33×10^{-5}	2.16×10^{-5}	Acceptable CR	1.53×10^{-5}	7.91×10^{-6}	Acceptable CR
	Pb	3.74×10^{-7}	3.14×10^{-7}	Negligible CR	1.72×10^{-7}	1.21×10^{-7}	Negligible CR
TCR	Total	4.99×10^{-5}	2.84×10^{-5}	Acceptable CR	2.46×10^{-5}	1.04×10^{-5}	Acceptable CR
Children/adult ratio	2.53						

[a] NCR = Non-Carcinogenic Risk, CR = Carcinogenic Risk.

However, the data for children indicated greater concern, with the 5th percentile TCR (1.82×10^{-4}) within acceptable limits, but the 95th percentile (1.06×10^{-4}) exceeding the significant cancer risk range. Notably, TCR showed a 100% probability of exceeding the acceptable CR threshold (10^{-6}) for both children and adults. More alarmingly, children exhibited a 5.52% chance of exceeding the significant CR threshold (10^{-4}), underscoring the heightened risk they face.

Ni was identified as posing the highest CR risk for both children and adults, with ILCR values of 3.33×10^{-5} (95% CI: 1.05×10^{-5}, 7.45×10^{-5}) and 1.53×10^{-5} (95% CI: 6.02×10^{-6}, 3.01×10^{-5}), respectively, falling within the acceptable range (Fig. 5n). The MCS results for Ni showed a 100% probability of exceeding the 10^{-6} threshold for both age groups, with children having a 1.66% chance of surpassing the 10^{-4} significant risk level. Cd (children = 1.42×10^{-6}; adults = 6.75×10^{-7}) and Cr (children = 1.52×10^{-5}; adults = 8.59×10^{-6}) also demonstrated acceptable CR risk (Fig. 5l and m). For Cd, children (35.87%) and adults (17.43%) both showed chances of exceeding the 10^{-6} threshold. For Cd, children (35.87%) and adults (17.43%) both showed chances of exceeding the acceptable risk threshold. Cr exhibited a 100% probability of exceeding the acceptable risk level for children and 99.99% for adults, with a slight chance of exceeding the significant risk level for children. The risk posed by Pb (children = 3.74×10^{-7}; adults = 1.72×10^{-7}) was comparatively lower, with only a 4.47% chance for children and merely zero chance for adults of exceeding the acceptable risk threshold (Fig. 5o). This finding suggested that continued exposure, particularly at higher levels, could markedly increase the cancer risk in children.[16]

The elevated susceptibility of children was further emphasized by the children/adult TCR ratio of 2.53, underscoring the heightened risk they face, especially through ingestion, where the risk was found to be 2.25 times greater than that for the adults. Conversely, adults were at higher risk than children through dermal contact (1.78 times) and inhalation (1.05 times) (Table S7). CR posed by Ni on children was 89.36 and 23.75 times higher than Pb and Cd, respectively. Similarly, for adults, the CR posed by Ni was 87.37 and 22.41 times higher than Pb and Cd, respectively.

The sensitivity analysis for NCR (Fig. 6a and Table S8) demonstrated average body weight (ABW) exerting a negative effect on HI estimation for both adults (−15.60%) and children (−5.60%). For children, exposed skin area (ESA) was the most significant factor, contributing 41.30% to the risk, followed by Fe concentration (23.80%), exposure frequency (EXF) (13.00%), and Mn concentration (12.00%). Cr and Pb exerted minimal influences at 4.00% and 3.80%, respectively. In contrast, for adults, Fe concentration was the most dominant factor, accounting for 39.70% of the risk, with Mn (18.90%), EXF (14.40%), and ESA (9.80%) also contributing significantly. Cr and Pb had minor impacts at 4.00% and 1.10%, respectively. In the CR analysis (Fig. 6b), different patterns emerged. For children, exposure duration (ED) was the most substantial factor, contributing 53.10% to the risk, followed by Ni concentration (27.70%), Cr concentration (8.00%), and EXF (7.30%). ABW again showed a negative effect, though smaller at −3.30%. In adults, Ni concentration was the most influential factor, contributing 44.70% to the risk, followed by Cr concentration (18.10%), EXF (13.00%), and ED (8.40%). The negative impact of ABW was more pronounced in adults (−14.70%) compared to children. The overall sensitivity result revealed significant differences in risk factors between adults and children, underscoring the necessity for age-specific risk management strategies. The prominent influence of ED on CR in children emphasizes the critical need to minimize long-term exposure.

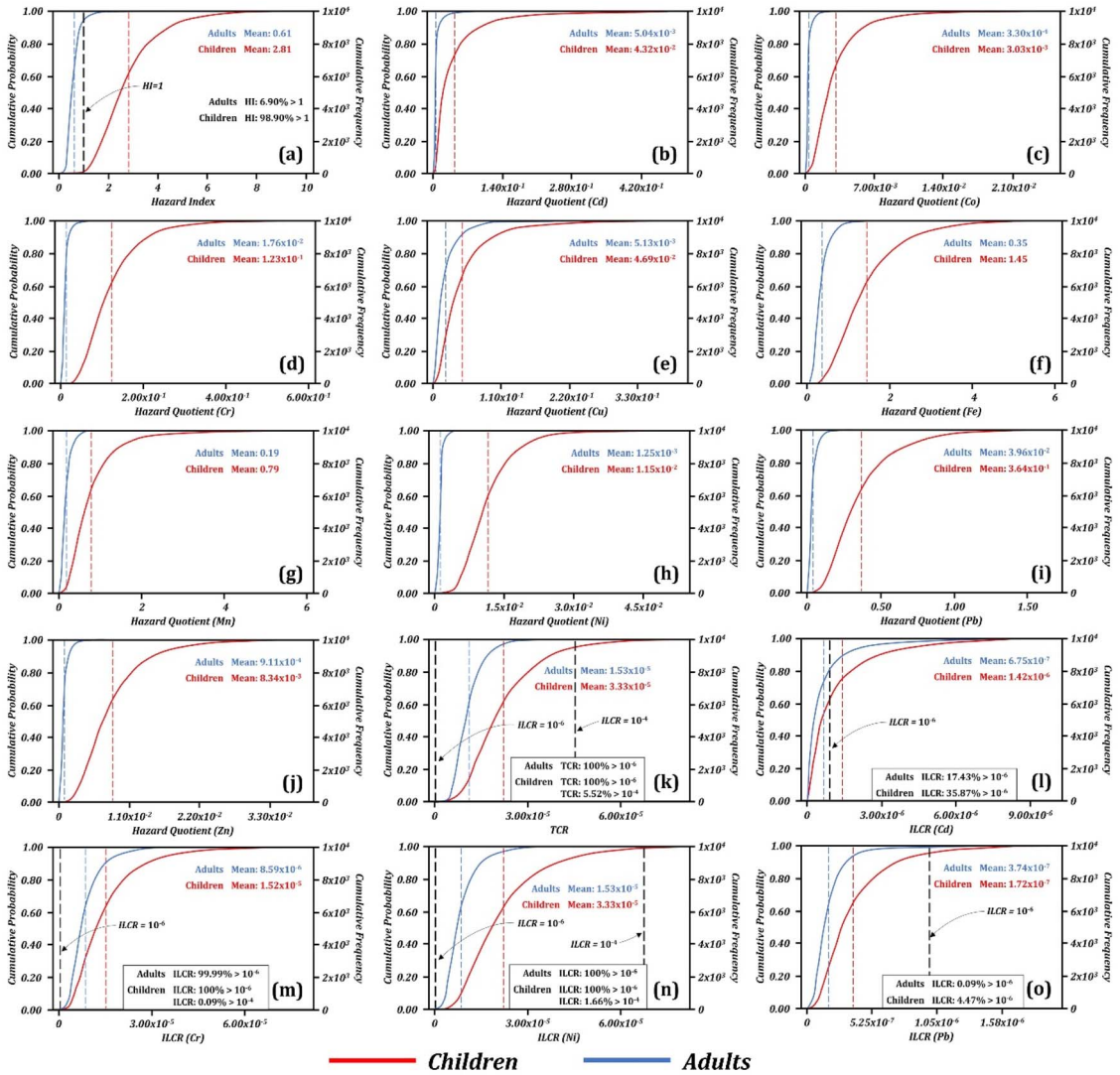

Fig. 5 MCS derived probability distributions for (a) the HI; and the HQs of (b) Cd, (c) Co, (d) Cu, (e) Cr, (f) Fe, (g) Mn, (h) Ni, (i) Pb, and (j) Zn. MCS derived probability distribution and percentage exceeding the thresholds of 10^{-6} and 10^{-4} for (k) TCR and for the ILCRs of (l) Cd, (m) Cr, (n) Ni, and (o) Pb. The red dashed lines indicate the mean values for children, and the blue dashed lines denote the average values for adults. The black lines represent the acceptable and significant CR levels (10^{-6} and 10^{-4}).

Furthermore, the consistent negative impact of ABW indicates that individuals with lower body weight, particularly children, are at heightened risk, underscoring the importance of protecting vulnerable populations. Efforts should be made on the importance of reducing skin contact and overall exposure time as effective mitigation strategies, particularly for children.

3.4. Insights on health risks coupled with the PMF model outcome

The PMF-HRA approach was employed in this study to appraise the health implications linked to diverse TE contamination sources. This methodology synergistically combines the PMF model with HRA techniques. Utilizing the source apportionment outcomes stemming from the PMF model, the relative contributions of distinct factors were subsequently applied to quantify both NCR and CR. The analysis, as depicted in Fig. 7, revealed that the proportional impact of various PMF factors on health risks exhibited comparable patterns across children and adults.

F_1, dominated by Cd, contributed minimally to both NCR and CR across all demographic groups, accounting for only 0.59% of NCR in children and 0.32% in adults. Its contribution to CR was similarly low, at 1.09% for children and 1.05% for adults. However, the cancer risk associated with Cd in children (1.42×10^{-6}) exceeded the acceptable limit, highlighting Cd as a potent toxin with profound health implications. Chronic exposure to Cd in children can lead to neurological dysfunction, cognitive impairment, DNA damage, and developmental delays, particularly in those with underdeveloped organs and systems.[161,162] Early exposure has been linked to lower IQ and reduced ingenuity, particularly in boys.[163,164] For adults, the cancer risk of 6.75×10^{-7} was slightly below the tolerable limit,

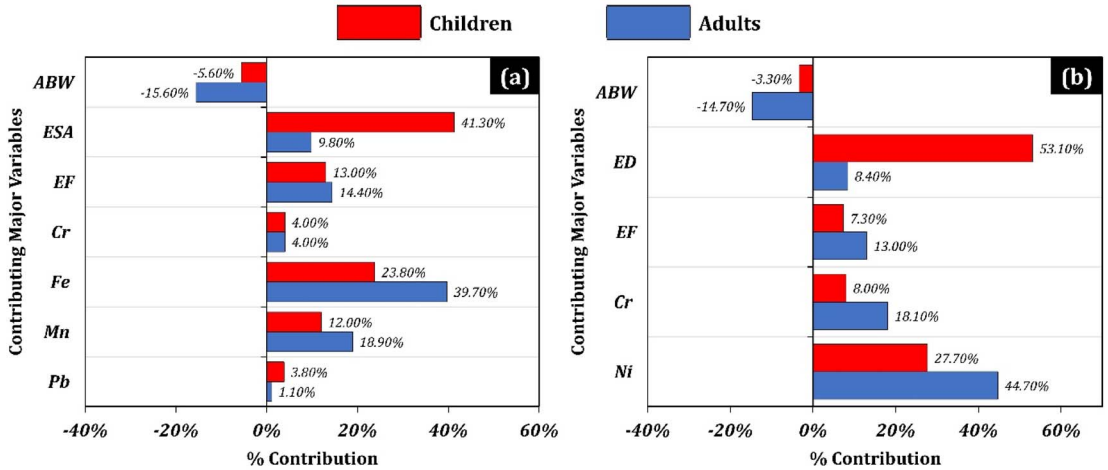

Fig. 6 Major contributing variables to the total (a) NCR and (b) CR for children and adults, based on sensitivity analysis from the MCS.

but chronic exposure can still result in severe health effects, including liver damage, respiratory disorders, and reduced life expectancy, especially in those with pre-existing conditions related to Cd.[165,166]

Interestingly, while F_2 was identified as predominantly natural and geogenic in origin, it emerged as the most significant contributor to health risks. This apparent contradiction can be attributed to the bio-accessibility and bioavailability of these F_2 TEs in the soil, as well as their essential yet potentially toxic dual role in human health. In terms of NCR, F_2 dominated with a contribution of 79.27% for children and 88.69% for adults, highlighting its critical role in elevating health risks. This trend continued with CR, where F_2 contributed 66.18% to children's risk and 61.63% to that of adults. Iron is essential for oxygen transport and metabolism, but excess Fe, particularly in children, can lead to conditions like hemosiderosis and hemochromatosis, potentially damaging the liver, heart, and pancreas.[167,168] Mn also poses significant NCRs, especially to the brain and lungs, with overexposure linked to neurological disorders similar to Parkinson's disease.[169] Co is necessary in small amounts but can cause respiratory issues and dermatitis at higher exposures.[170,171] Among F_2 metals, only Ni is classified

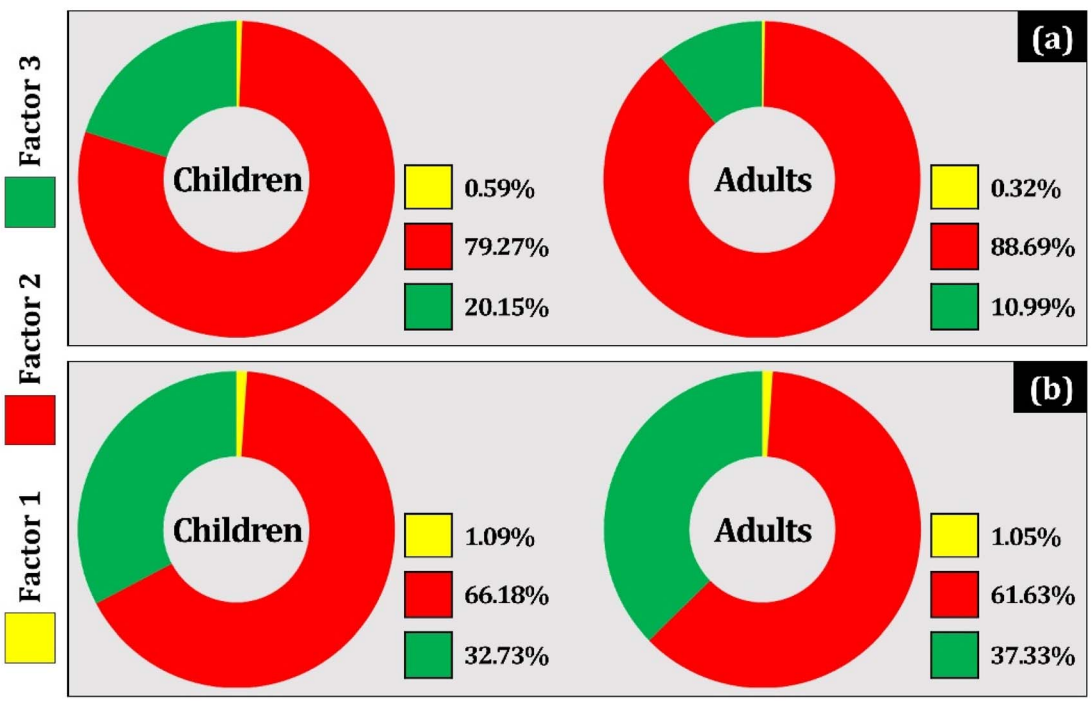

Fig. 7 Comparison of health risks associated with identified PMF factor groups of TEs: (a) NCR and (b) CR in children and adults from the PMF-HRA model.

as a carcinogen in typical exposure scenarios.[172] While Ni contributes minimally to NCR, it is a significant carcinogenic threat, linked to lung and nasal cancers.[173] Nickel is also a common cause of contact allergies, particularly in children, and maternal exposure has been associated with congenital heart defects.[174,175]

F_3, encompassing Cr, Cu, Pb, and Zn, emerged as a significant contributor to exposure risks, particularly among children. Specifically, it accounted for 20.15% of the NCR in children, compared to 10.99% in adults. Although F_3 is less predominant than F_2, it still warrants considerable attention, especially given its disproportionate impact on younger populations. Regarding CR, F_3 exerted a more pronounced effect on adults, contributing 37.33% to their overall risk, compared to 32.73% for children. Though the NCR associated with F_3 remained within acceptable thresholds, the CR assessment revealed significant concerns, particularly with respect to hexavalent chromium (Cr VI), a well-known respiratory carcinogen. Environmental exposure to Cr VI is linked to severe health consequences, including adverse pregnancy outcomes and heightened respiratory issues in children.[176,177] In this study, Cr VI posed a cancer risk to children that was 1.78 times greater than that for adults, whereas the CR from Pb was deemed negligible. Chronic Pb exposure is also a critical public health concern, especially for children, as it can lead to systemic health effects, including intellectual disabilities and developmental delays.[178,179] Elevated soil Pb levels, particularly in areas adjacent to dumpsites, have been correlated with increased blood Pb levels in children, underscoring the pressing need for targeted interventions in polluted regions.[180,181]

In summary, F_2 stood out as the most significant contributor to both NCR and CR, particularly for adults. F_3, while less dominant, still posed a considerable risk, especially for children, due to their increased sensitivity to TE exposure. F_1, although present, contributed minimally to overall health risks. These findings underscored the need for targeted interventions that focus on reducing exposure to the metals associated with Factors 2 and 3, especially for children due to their high vulnerability.

4. Limitations of the study and scope for future research

In this study, efforts were made to assess TE contamination, its sources, and associated health risks, but several noteworthy limitations must be addressed. Firstly, a detailed waste characterization of the dumpsite was not undertaken. Previous research in a developing nation revealed that biodegradable materials from households, markets, roadside eateries, and hotels constitute a substantial portion (56.30%) of solid waste at such sites.[182] A comprehensive waste characterization could have offered a more precise insight into the sources contributing to the waste. Secondly, although some other TEs commonly identified in prior dumpsite contamination investigations,[183,184] including arsenic (As), mercury (Hg), and antimony (Sb), are significant concerns, their omission in our analysis resulted from analytical constraints. Expanding the elemental scope may have provided a more comprehensive analysis of contamination risk. Thirdly, there is considerable variability in the reference values employed for evaluating soil TE concentrations. This study utilized background values as consistent reference points; however, alternative approaches in other studies have included the use of pre-industrial reference levels, average crustal concentrations, or typical shale content.[39,50] The selection of reference values is a critical factor that can substantially influence the accuracy of the assessment outcomes. Moreover, the appraisal of NCR and CR linked to the exposure to target TEs in soil was limited to three key pathways: oral ingestion, inhalation, and dermal absorption. This limitation arose from the lack of available data on the local population's dietary habits. Consequently, the analysis excluded other significant exposure routes like food and water consumption, which could potentially lead to an underestimation of the total health risks. Finally, due to the absence of local data on exposure parameters, the study relied on the USEPA's standardized exposure values and probability distributions for risk calculations and simulations. While this approach helped mitigate the lack of regional data, it introduces a limitation as the applied values may not fully represent local environmental and population-specific conditions, potentially affecting the precision of the risk estimates.

While the largest landfill in the Feni municipality was assessed in the current study, there are numerous smaller dumpsites scattered both within and outside the municipal boundaries. Future studies that incorporate these areas could provide a more comprehensive assessment of contamination levels and health risk characterization on a larger scale. Additionally, the temporal dimension of TE pollution was not addressed in this study. Given that factors such as seasonal changes, climate conditions, and waste composition impact the environmental breakdown and transformation of TEs,[185,186] it is crucial to conduct longitudinal studies that track changes in contamination levels over time. This would offer an important understanding of the temporal patterns and enduring effects of TE contamination. Moreover, utilizing more advanced analytical methods, such as isotopic analysis, can significantly enhance the precision of source apportionment of TEs within the soil and aid in formulating more effective mitigation strategies.[20] Finally, future studies should consider the synergistic effects of multiple contaminants and their bioaccumulation in the food chain, as well as the potential for groundwater contamination.

5. Conclusions

This study was conducted to evaluate the significant environmental and public health challenges posed by TEs in the DSS due to ongoing waste burning, an issue that has remained inadequately investigated since the onset of burning approximately 25 years ago, making this research both timely and essential. The contamination indices, PMF, and PCM results revealed that Cd, Cu, Zn, Pb, and Cr were primarily influenced by anthropogenic activities like industrial and residential waste,

while Fe, Co, Mn, and Ni indicated geogenic origins, with localized hotspots linked to waste processing. PMF identified three factors: F_1 (Cd-dominated, 82.26%), F_2 (Fe, Co, Mn, Ni), and F_3 (Cu, Zn, Pb, Cr), highlighting the complexity of pollution sources. Despite low concentrations, Cd showed extreme contamination, linked to industrial waste, contributing to 91% of the total ecological risks at the dumpsite, and exhibiting the highest contamination indices. The results indicated moderate-to-severe contamination in the DSS, with Cd, due to its high toxicity, posing the most severe ecological risks among all TEs. Meanwhile, F_3 reflected significant contributions from residential and commercial waste, as well as vehicular emissions, further highlighting the complexity of pollution sources.

According to the PMF-HRA model, used for concentration- and source-oriented HRA, children had higher NCR and CR than adults. The HI for children (2.81) exceeded the safe threshold, primarily driven by Fe and Mn, while adults had a lower HI (0.61). Inhalation was the dominant pathway for NCR, contributing 67.26% and 78.36% to the total HI for children and adults, respectively. For CR, the ILCR for children (4.99×10^{-5}) and adults (2.46×10^{-5}) exceeded the acceptable range (10^{-6}), with Ni posing the highest risk (children: 3.33×10^{-5}; adults: 1.53×10^{-5}). Cd and Cr also contributed significantly, with Cd exceeding acceptable CR limits for children (1.42×10^{-6}). PMF identified F_2 as the largest contributor to both NCR (79.27% in children; 88.69% in adults) and CR (66.18% in children; 61.63% in adults), while F_3 posed considerable risks, particularly for children.

Given the proximity of the dumpsite to residential areas, agricultural lands, and transportation infrastructure, this study highlights the urgent need for targeted interventions to mitigate TE exposure, particularly in children, who are more vulnerable due to their developmental stage and higher exposure rates. The PMF-HRA approach effectively linked pollution sources to health risks, providing a framework for prioritizing mitigation efforts. Immediate remediation and sustainable waste management strategies are essential to prevent further contamination. Regular monitoring of soil and air quality, stricter regulation of major pollution sources, and community awareness programs will be critical in reducing exposure risks. As inhalation remains the primary exposure pathway, atmospheric controls should be prioritized to minimize health impacts. Given the persistence and bioaccumulation potential of these TEs, long-term monitoring and policy interventions are necessary to protect vulnerable populations.

Author contributions

Hrithik Nath: conceptualization, methodology, investigation, data curation, software, validation, formal analysis, writing – original draft, writing – review & editing, visualization. Sajal Kumar Adhikary: methodology, writing – review & editing, supervision. Srabanti Roy: methodology, investigation, writing – original draft. Sunjida Akhter: methodology, investigation, formal analysis. Ummey Hafsa Bithi: methodology, investigation, writing – review & editing. Mohammed Abdus Salam: validation, writing – review & editing. Abu Reza Md. Towfiqul Islam: visualization, writing – review & editing. Md. Abu Bakar Siddique: conceptualization, methodology, investigation, formal analysis, data curation, validation, writing – review & editing, visualization, supervision. All authors read and approved of the final manuscript.

Conflicts of interest

There are no conflicts of interest to declare.

Data availability

Data will be made available on request.

Supplementary information is available. See DOI: https://doi.org/10.1039/d5va00141b.

Acknowledgements

The authors would like to thank the following individuals for their support in gathering soil data for the study: Md. Abu Faysal, Md. Al Arman Chowdhury, Md. Jubayer, Md. Khales Ahamed Roxy, Md. Rashedul Islam, Md. Sazzad Hossain, Mohammed Arif Hossen, NKM Munna Talukder, and Raju Devnath. The authors acknowledge the analytical laboratory support of the Institute of National Analytical Research and Service (INARS), Bangladesh Council of Scientific and Industrial Research (BCSIR), Dhaka, Bangladesh.

References

1 I. Khan, S. Chowdhury and K. Techato, Waste to Energy in Developing Countries—A Rapid Review: Opportunities, Challenges, and Policies in Selected Countries of Sub-Saharan Africa and South Asia towards Sustainability, *Sustainability*, 2022, **14**(7), 3740.

2 K. G. B. Awuah and R. T. Abdulai, Urban Land and Development Management in a Challenged Developing World: An Overview of New Reflections, *Land*, 2022, **11**(1), 129.

3 F. Ahmed, S. Hasan, M. S. Rana and N. Sharmin, A conceptual framework for zero waste management in Bangladesh, *Int. J. Environ. Sci. Technol.*, 2023, **20**(2), 1887–1904.

4 S. O. Kwakye, E. E. Y. Amuah, K. A. Ankoma, E. B. Agyemang and B. G. Owusu, Understanding the performance and challenges of solid waste management in an emerging megacity: Insights from the developing world, *Environ. Chall.*, 2024, **14**, 100805.

5 B. S. Ramadan, I. Rachman, N. Ikhlas, S. B. Kurniawan, M. F. Miftahadi and T. Matsumoto, A comprehensive review of domestic-open waste burning: recent trends, methodology comparison, and factors assessment, *J. Mater. Cycles Waste Manag.*, 2022, **24**(5), 1633–1647, DOI: 10.1007/s10163-022-01430-9.

6 J. Wei, H. Li and J. Liu, Heavy metal pollution in the soil around municipal solid waste incinerators and its health risks in China, *Environ. Res.*, 2022, **203**, 111871. Available

from: https://linkinghub.elsevier.com/retrieve/pii/S0013935121011658.
7 N. Ferronato and V. Torretta, Waste Mismanagement in Developing Countries: A Review of Global Issues, *Int. J. Environ. Res. Publ. Health*, 2019, **16**(6), 1060.
8 W. Yao, Y. Zhao, R. Chen, M. Wang, W. Song and D. Yu, Emissions of Toxic Substances from Biomass Burning: A Review of Methods and Technical Influencing Factors, *Processes*, 2023, **11**(3), 853.
9 W. Ahmad, R. D. Alharthy, M. Zubair, M. Ahmed, A. Hameed and S. Rafique, Toxic and heavy metals contamination assessment in soil and water to evaluate human health risk, *Sci. Rep.*, 2021, **11**(1), 17006.
10 M. Hussein, K. Yoneda, Z. Mohd-Zaki, A. Amir and N. Othman, Heavy metals in leachate, impacted soils and natural soils of different landfills in Malaysia: An alarming threat, *Chemosphere*, 2021, **267**, 128874.
11 X. Bo, J. Guo, R. Wan, Y. Jia, Z. Yang, Y. Lu, *et al.*, Characteristics, correlations and health risks of PCDD/Fs and heavy metals in surface soil near municipal solid waste incineration plants in Southwest China, *Environ. Pollut.*, 2022, **298**, 118816.
12 P. J. Jannetto and C. T. Cowl, Elementary Overview of Heavy Metals, *Clin. Chem.*, 2023, **69**(4), 336–349.
13 M. Balali-Mood, K. Naseri, Z. Tahergorabi, M. R. Khazdair and M. Sadeghi, Toxic Mechanisms of Five Heavy Metals: Mercury, Lead, Chromium, Cadmium, and Arsenic, *Front. Pharmacol*, 2021, **12**, 643972.
14 A. V. Skalny, T. R. R. Lima, T. Ke, J. C. Zhou, J. Bornhorst, S. I. Alekseenko, *et al.*, Toxic metal exposure as a possible risk factor for COVID-19 and other respiratory infectious diseases, *Food Chem. Toxicol.*, 2020, **146**, 111809. Available from: https://linkinghub.elsevier.com/retrieve/pii/S0278691520306992.
15 H. Hossini, B. Shafie, A. D. Niri, M. Nazari, A. J. Esfahlan, M. Ahmadpour, *et al.*, A comprehensive review on human health effects of chromium: insights on induced toxicity, *Environ. Sci. Pollut. Res.*, 2022, **29**(47), 70686–70705, DOI: 10.1007/s11356-022-22705-6.
16 S. Karimian, S. Shekoohiyan and G. Moussavi, Health and ecological risk assessment and simulation of heavy metal-contaminated soil of Tehran landfill, *RSC Adv.*, 2021, **11**(14), 8080–8095. Available from: https://xlink.rsc.org/?DOI=D0RA08833A.
17 A. S. Kolawole and A. O. Iyiola, Environmental Pollution: Threats, Impact on Biodiversity, and Protection Strategies, in *Sustainable utilization and conservation of Africa's biological resources and environment*, Springer Nature Singapore, Singapore, 2023, pp. 377–409, DOI: 10.1007/978-981-19-6974-4_14.
18 J. M. Pedram, A. Kamali, H. Khara, N. Pourang and S. P. H. Shekarabi, Microplastic pollution and heavy metal risk assessment in Perca fluviatilis from Anzali wetland: Implications for environmental health and human consumption, *Sci. Total Environ.*, 2024, **907**, 167978. Available from: https://linkinghub.elsevier.com/retrieve/pii/S0048969723066056.
19 S. Coelho, J. Ferreira, V. Rodrigues and M. Lopes, Source apportionment of air pollution in European urban areas: Lessons from the ClairCity project, *J. Environ. Manage.*, 2022, **320**, 115899.
20 Y. Wang, Y. Li, S. Yang, J. Liu, W. Zheng, J. Xu, *et al.*, Source apportionment of soil heavy metals: A new quantitative framework coupling receptor model and stable isotopic ratios, *Environ. Pollut.*, 2022, **314**, 120291.
21 J. Huang, S. Guo, G. m. Zeng, F. Li, Y. Gu, Y. Shi, *et al.*, A new exploration of health risk assessment quantification from sources of soil heavy metals under different land use, *Environ. Pollut.*, 2018, **243**, 49–58.
22 L. Zhou, X. Zhao, Y. Meng, Y. Fei, M. Teng, F. Song, *et al.*, Identification priority source of soil heavy metals pollution based on source-specific ecological and human health risk analysis in a typical smelting and mining region of South China, *Ecotoxicol. Environ. Saf.*, 2022, **242**, 113864.
23 H. H. Jiang, L. M. Cai, G. C. Hu, H. H. Wen, J. Luo, H. Q. Xu, *et al.*, An integrated exploration on health risk assessment quantification of potentially hazardous elements in soils from the perspective of sources, *Ecotoxicol. Environ. Saf.*, 2021, **208**, 111489.
24 H. Chen, D. Wu, Q. Wang, L. Fang, Y. Wang, C. Zhan, *et al.*, The Predominant Sources of Heavy Metals in Different Types of Fugitive Dust Determined by Principal Component Analysis (PCA) and Positive Matrix Factorization (PMF) Modeling in Southeast Hubei: A Typical Mining and Metallurgy Area in Central China, *Int. J. Environ. Res. Publ. Health*, 2022, **19**(20), 13227.
25 W. Du, P. Zeng, S. Yu, F. Liu and P. Sun, Distribution, Risk Assessment, and Quantitative Source Analysis of Soil Heavy Metals in a Typical Agricultural City of East-Central China, *Land*, 2025, **14**(1), 66.
26 H. El Fadili, M. Ben Ali, M. N. Rahman, M. El Mahi, E. M. Lotfi and S. Louki, Bioavailability and health risk of pollutants around a controlled landfill in Morocco: Synergistic effects of landfilling and intensive agriculture, *Heliyon*, 2024, **10**(1), e23729.
27 J. Liang, Z. Liu, Y. Tian, H. Shi, Y. Fei, J. Qi, *et al.*, Research on health risk assessment of heavy metals in soil based on multi-factor source apportionment: A case study in Guangdong Province, China, *Sci. Total Environ.*, 2023, **858**, 159991.
28 M. Taghavi, K. Bakhshi, A. Zarei, E. Hoseinzadeh and A. Gholizadeh, Soil pollution indices and health risk assessment of metal(loid)s in the agricultural soil of pistachio orchards, *Sci. Rep.*, 2024, **14**(1), 8971.
29 V. Upadhyay, A. Kumari and S. Kumar, From soil to health hazards: Heavy metals contamination in northern India and health risk assessment, *Chemosphere*, 2024, **354**, 141697.
30 S. Yang, J. Zhao, S. X. Chang, C. Collins, J. Xu and X. Liu, Status assessment and probabilistic health risk modeling of metals accumulation in agriculture soils across China: A synthesis, *Environ. Int.*, 2019, **128**, 165–174.

31 M. M. Orosun, A. D. Adewuyi, N. B. Salawu, M. O. Isinkaye, O. R. Orosun and A. S. Oniku, Monte Carlo approach to risks assessment of heavy metals at automobile spare part and recycling market in Ilorin, Nigeria, *Sci. Rep.*, 2020, **10**(1), 22084.
32 Q. Yang, L. Zhang, H. Wang and J. D. Martín, Bioavailability and health risk of toxic heavy metals (As, Hg, Pb and Cd) in urban soils: A Monte Carlo simulation approach, *Environ. Res.*, 2022, **214**, 113772.
33 J. Huang, Y. Wu, J. Sun, X. Li, X. Geng, M. Zhao, *et al.*, Health risk assessment of heavy metal(loid)s in park soils of the largest megacity in China by using Monte Carlo simulation coupled with Positive matrix factorization model, *J. Hazard. Mater.*, 2021, **415**, 125629.
34 H. Luo, P. Wang, Q. Wang, X. Lyu, E. Zhang, X. Yang, *et al.*, Pollution sources and risk assessment of potentially toxic elements in soils of multiple land use types in the arid zone of Northwest China based on Monte Carlo simulation, *Ecotoxicol. Environ. Saf.*, 2024, **279**, 116479.
35 BBS, *Population and Housing Census*, Bangladesh Bureau of Statistics (BBS), 2022.
36 A. Azam, *Feni Starts Producing Fertiliser from Garbage*, The Business Standard, 2021.
37 ETV, *Garbage Is Dumped at the Entrance of Feni Town*, Ekushey Television Limited, 2018.
38 ITV, *Residents of the Two Municipal Areas Are Fed up with the Stench of Garbage*, Indipendent Television Limited, 2018.
39 J. N. Ihedioha, P. O. Ukoha and N. R. Ekere, Ecological and human health risk assessment of heavy metal contamination in soil of a municipal solid waste dump in Uyo, Nigeria, *Environ. Geochem. Health*, 2017, **39**(3), 497–515.
40 T. Kormoker, R. Proshad, S. Islam, S. Ahmed, K. Chandra, M. Uddin, *et al.*, Toxic metals in agricultural soils near the industrial areas of Bangladesh: ecological and human health risk assessment, *Toxin Rev.*, 2021, **40**(4), 1135–1154.
41 I. A. R. M. Towfiqul, M. Hasanuzzaman, H. M. Touhidul Islam, M. U. Mia, R. Khan, M. A. Habib, *et al.*, Quantifying Source Apportionment, Co-occurrence, and Ecotoxicological Risk of Metals from Upstream, Lower Midstream, and Downstream River Segments, Bangladesh, *Environ. Toxicol. Chem.*, 2020, **39**(10), 2041–2054.
42 A. B. Hasan, A. H. M. S. Reza, S. Kabir, M. A. B. Siddique, M. A. Ahsan and M. A. Akbor, Accumulation and distribution of heavy metals in soil and food crops around the ship breaking area in southern Bangladesh and associated health risk assessment, *SN Appl. Sci.*, 2020, **2**(2), 155.
43 M. A. Akbor, M. M. Rahman, M. Bodrud-Doza, M. M. Haque, M. A. B. Siddique, M. A. Ahsan, *et al.*, Metal pollution in water and sediment of the Buriganga River, Bangladesh: an ecological risk perspective, *Desalination Water Treat.*, 2020, **193**, 284–301.
44 V. C. Eze, V. Onwukeme and C. E. Enyoh, Pollution status, ecological and human health risks of heavy metals in soil from some selected active dumpsites in Southeastern, Nigeria using energy dispersive X-ray spectrometer, *Int. J. Environ. Anal. Chem.*, 2022, **102**(16), 3722–3743.
45 P. Saha, K. Kumar Saikia, M. Kumar and S. Handique, Assessment of health risk and pollution load for heavy and toxic metal contamination from leachate in soil and groundwater in the vicinity of dumping site in Mid-Brahmaputra Valley, India, *Total Environ. Res. Themes*, 2023, **8**, 100076.
46 P. Ilić, S. Ilić, Z. Mushtaq, A. Rashid, LjS. Bjelić, D. N. Markić, *et al.*, Assessing the Ecological Risks and Spatial Distribution of Heavy Metal Contamination at Solid Waste Dumpsites, *Eurasian Soil Sci.*, 2024, **57**(7), 1277–1296.
47 M. A. Ahsan, F. Satter, M. A. B. Siddique, M. A. Akbor, S. Ahmed, M. Shajahan, *et al.*, Chemical and physicochemical characterization of effluents from the tanning and textile industries in Bangladesh with multivariate statistical approach, *Environ. Monit. Assess.*, 2019, **191**(9), 575.
48 H. Z. Wang, L. M. Cai, Q. S. Wang, G. C. Hu and L. G. Chen, A comprehensive exploration of risk assessment and source quantification of potentially toxic elements in road dust: A case study from a large Cu smelter in central China, *Catena*, 2021, **196**, 104930.
49 U. Förstner, W. Ahlf, W. Calmano and M. Kersten, *Sediments and Environmental Geochemistry*, ed. D. Heling, P. Rothe, U. Förstner, P. Stoffers, Springer Berlin Heidelberg, Berlin, Heidelberg, 1990.
50 L. Hakanson, An ecological risk index for aquatic pollution control.a sedimentological approach, *Water Res.*, 1980, **14**(8), 975–1001.
51 S. L. C. Ferreira, J. B. da Silva, I. F. dos Santos, O. M. C. de Oliveira, V. Cerda and A. F. S. Queiroz, Use of pollution indices and ecological risk in the assessment of contamination from chemical elements in soils and sediments – Practical aspects, *Trends Environ. Anal. Chem.*, 2022, **35**, e00169.
52 F. Ustaoğlu, Y. Tepe and H. Aydin, Heavy metals in sediments of two nearby streams from Southeastern Black Sea coast: Contamination and ecological risk assessment, *Environ. Forensics*, 2020, **21**(2), 145–156.
53 C. Reimann and P. de Caritat, Distinguishing between natural and anthropogenic sources for elements in the environment: regional geochemical surveys versus enrichment factors, *Sci. Total Environ.*, 2005, **337**(1–3), 91–107.
54 A. O. Adelopo, P. I. Haris, B. I. Alo, K. Huddersman and R. O. Jenkins, Multivariate analysis of the effects of age, particle size and landfill depth on heavy metals pollution content of closed and active landfill precursors, *Waste Manage.*, 2018, **78**, 227–237.
55 M. Sabir, E. Baltrėnaitė-Gedienė, A. Ditta, H. Ullah, A. Kanwal, S. Ullah, *et al.*, Bioaccumulation of Heavy Metals in a Soil–Plant System from an Open Dumpsite and the Associated Health Risks through Multiple Routes, *Sustainability*, 2022, **14**(20), 13223.

56 L. O. Afolagboye, A. A. Ojo and A. O. Talabi, Evaluation of soil contamination status around a municipal waste dumpsite using contamination indices, soil-quality guidelines, and multivariate statistical analysis, *SN Appl. Sci.*, 2020, **2**(11), 1864.
57 M. A. H. Bhuiyan, L. Parvez, M. A. Islam, S. B. Dampare and S. Suzuki, Heavy metal pollution of coal mine-affected agricultural soils in the northern part of Bangladesh, *J. Hazard. Mater.*, 2010, **173**(1–3), 384–392.
58 C. J. Tomlinson, L. Chapman, J. E. Thornes and C. J. Baker, Including the urban heat island in spatial heat health risk assessment strategies: A case study for Birmingham, UK, *Int. J. Health Geogr.*, 2011, **10**(1), 42.
59 G. O. Duodu, K. N. Ogogo, S. Mummullage, F. Harden, A. Goonetilleke and G. A. Ayoko, Source apportionment and risk assessment of PAHs in Brisbane River sediment, Australia, *Ecol. Indic.*, 2017, **73**, 784–799.
60 N. Yan, W. Liu, H. Xie, L. Gao, Y. Han, M. Wang, *et al.*, Distribution and assessment of heavy metals in the surface sediment of Yellow River, China, *J. Environ. Sci.*, 2016, **39**, 45–51.
61 M. C. Avendaño, M. E. Palomeque, P. Roqué, A. Lojo and M. Garrido, Spatiotemporal distribution and human health risk assessment of potential toxic species in soils of urban and surrounding crop fields from an agricultural area, Córdoba, Argentina, *Environ. Monit. Assess.*, 2021, **193**(10), 661.
62 L. Luo, K. Mei, L. Qu, C. Zhang, H. Chen, S. Wang, *et al.*, Assessment of the Geographical Detector Method for investigating heavy metal source apportionment in an urban watershed of Eastern China, *Sci. Total Environ.*, 2019, **653**, 714–722.
63 H. Liu, Y. Wang, J. Dong, L. Cao, L. Yu and J. Xin, Distribution Characteristics, Pollution Assessment, and Source Identification of Heavy Metals in Soils Around a Landfill-Farmland Multisource Hybrid District, *Arch. Environ. Contam. Toxicol.*, 2021, **81**(1), 77–90, DOI: 10.1007/s00244-021-00857-9.
64 Y. Huang, T. Li, C. Wu, Z. He, J. Japenga, M. Deng, *et al.*, An integrated approach to assess heavy metal source apportionment in peri-urban agricultural soils, *J. Hazard. Mater.*, 2015, **299**, 540–549.
65 U. K. Singh and B. Kumar, Pathways of heavy metals contamination and associated human health risk in Ajay River basin, India, *Chemosphere*, 2017, **174**, 183–199.
66 P. Govender and V. Sivakumar, Application of k-means and hierarchical clustering techniques for analysis of air pollution: A review (1980–2019), *Atmos. Pollut. Res.*, 2020, **11**(1), 40–56.
67 Y. Jiang, H. Guo, Y. Jia, Y. Cao and C. Hu, Principal component analysis and hierarchical cluster analyses of arsenic groundwater geochemistry in the Hetao basin, Inner Mongolia, *Geochemistry*, 2015, **75**(2), 197–205.
68 B. Yüksel, F. Ustaoğlu, C. Tokatli and M. S. Islam, Ecotoxicological risk assessment for sediments of Çavuşlu stream in Giresun, Turkey: association between garbage disposal facility and metallic accumulation, *Environ. Sci. Pollut. Res.*, 2022, **29**(12), 17223–17240.
69 M. S. Islam, M. B. Hossain, A. Matin and M. S. Islam Sarker, Assessment of heavy metal pollution, distribution and source apportionment in the sediment from Feni River estuary, Bangladesh, *Chemosphere*, 2018, **202**, 25–32.
70 F. Ustaoğlu and M. S. Islam, Potential toxic elements in sediment of some rivers at Giresun, Northeast Turkey: A preliminary assessment for ecotoxicological status and health risk, *Ecol. Indic.*, 2020, **113**, 106237.
71 X. Y. Zhou and X. R. Wang, Impact of industrial activities on heavy metal contamination in soils in three major urban agglomerations of China, *J. Clean. Prod.*, 2019, **230**, 1–10.
72 Y. Liu, Q. Du, Q. Wang, H. Yu, J. Liu, Y. Tian, *et al.*, Causal inference between bioavailability of heavy metals and environmental factors in a large-scale region, *Environ. Pollut.*, 2017, **226**, 370–378.
73 G. Norris, R. Duvall, S. Brown and S. Bai, *EPA Positive Matrix Factorization (PMF) 5.0 Fundamentals and User Guide*, EPA/600/R-14/108, United States Environmental Protection Agency, Washington, DC, USA, 2014.
74 Y. Jiang, S. Chao, J. Liu, Y. Yang, Y. Chen, A. Zhang, *et al.*, Source apportionment and health risk assessment of heavy metals in soil for a township in Jiangsu Province, China, *Chemosphere*, 2017, **168**, 1658–1668.
75 H. Liu, S. Anwar, L. Fang, L. Chen, W. Xu, L. Xiao, *et al.*, Source Apportionment of Agricultural Soil Heavy Metals Based on PMF Model and Multivariate Statistical Analysis, *Environ. Forensics*, 2024, **25**(1–2), 40–48.
76 W. Cheng, S. Lei, Z. Bian, Y. Zhao, Y. Li and Y. Gan, Geographic distribution of heavy metals and identification of their sources in soils near large, open-pit coal mines using positive matrix factorization, *J. Hazard. Mater.*, 2020, **387**, 121666.
77 C. Men, R. Liu, Q. Wang, L. Guo, Y. Miao and Z. Shen, Uncertainty analysis in source apportionment of heavy metals in road dust based on positive matrix factorization model and geographic information system, *Sci. Total Environ.*, 2019, **652**, 27–39.
78 Z. Y. Wu, L. N. Zhang, T. X. Xia, X. Y. Jia, H. Y. Li and S. J. Wang, Quantitative assessment of human health risks based on soil heavy metals and PAHs sources: take a polluted industrial site of beijing as an example, *Huan Jing Ke Xue*, 2020, **41**(9), 4180–4196.
79 X. Fei, Z. Lou, R. Xiao, Z. Ren and X. Lv, Contamination assessment and source apportionment of heavy metals in agricultural soil through the synthesis of PMF and GeogDetector models, *Sci. Total Environ.*, 2020, **747**, 141293.
80 Z. Pilková, L. Filová, E. Hiller and M. Mihaljevič, Re-Interpretation of Metal(Loid) Concentrations in Urban Soils of Two Different Land Uses by Positive Matrix Factorisation, *Environ. Forensics*, 2024, 626–644.
81 Q. Guan, R. Zhao, N. Pan, F. Wang, Y. Yang and H. Luo, Source apportionment of heavy metals in farmland soil of Wuwei, China: Comparison of three receptor models, *J. Clean. Prod.*, 2019, **237**, 117792.

82 Z. Q. Xu, S. J. Ni, X. G. Tuo and C. J. Zhang, Calculation of heavy metals' toxicity coefficient in the evaluation of potential ecological risk index, *Environ. Sci. Technol.*, 2008, **31**(2), 112–115.
83 C. T. Vu, C. Lin, C. C. Shern, G. Yeh, V. G. Le and H. T. Tran, Contamination, ecological risk and source apportionment of heavy metals in sediments and water of a contaminated river in Taiwan, *Ecol. Indic.*, 2017, **82**, 32–42.
84 A. Pejman, G. Nabi Bidhendi, M. Ardestani, M. Saeedi and A. Baghvand, A new index for assessing heavy metals contamination in sediments: A case study, *Ecol. Indic.*, 2015, **58**, 365–373.
85 N. Gujre, L. Rangan and S. Mitra, Occurrence, geochemical fraction, ecological and health risk assessment of cadmium, copper and nickel in soils contaminated with municipal solid wastes, *Chemosphere*, 2021, **271**, 129573.
86 S. Mishra, R. N. Bharagava, N. More, A. Yadav, S. Zainith, S. Mani, *et al.*, Heavy Metal Contamination: An Alarming Threat to Environment and Human Health, in *Environmental Biotechnology: for Sustainable Future*, Springer Singapore, Singapore, 2019, pp. 103–125.
87 H. Ali, E. Khan and I. Ilahi, Environmental Chemistry and Ecotoxicology of Hazardous Heavy Metals: Environmental Persistence, Toxicity, and Bioaccumulation, *J. Chem.*, 2019, **2019**, 1–14.
88 H. Nath and I. M. Rafizul, Spatial Variability of Metal Elements in Soils of a Waste Disposal Site in Khulna: A Geostatistical Study, *Adv. Civ. Eng.*, 2022, 25–36.
89 USEPA, *Risk Assessment Guidance for Superfund: Pt. A. Human Health Evaluation Manual*, Office of Emergency and Remedial Response, US Environmental Protection Agency, 1989, vol. 1.
90 USEPA, *Soil Screening Guidance: Technical Background Document*, EPA/540/R-95/128, Office of Soild Waste and Emergency Response, US Environmental Protection Agency, 1996.
91 L. T. Ogundele, I. A. Adejoro and P. O. Ayeku, Health risk assessment of heavy metals in soil samples from an abandoned industrial waste dumpsite in Ibadan, Nigeria, *Environ. Monit. Assess.*, 2019, **191**(5), 290.
92 USEPA, *Exposure Factors Handbook: 2011 Edition*, EPA/600/R-09/052F, National Center for Environmental Assessment, Office of Research and Development, Washington, DC, 2011.
93 IARC, Some Metals and Metallic Compounds, *IARC Monographs on the Evaluation of Carcinogenic Risks to Humans*, World Health Organization, Geneva, 1980.
94 R. Song, L. Liu, N. Wei, X. Li, J. Liu, J. Yuan, *et al.*, Short-term exposure to air pollution is an emerging but neglected risk factor for schizophrenia: A systematic review and meta-analysis, *Sci. Total Environ.*, 2023, **854**, 158823.
95 S. Thongyuan, T. Khantamoon, P. Aendo, A. Binot and P. Tulayakul, Ecological and health risk assessment, carcinogenic and non-carcinogenic effects of heavy metals contamination in the soil from municipal solid waste landfill in Central, Thailand, *Hum. Ecol. Risk Assess.: Int. J.*, 2021, **27**(4), 876–897, DOI: **10.1080/10807039.2020.1786666**.
96 L. L. Pham, S. J. Borghoff and C. M. Thompson, Comparison of threshold of toxicological concern (TTC) values to oral reference dose (RfD) values, *Regul. Toxicol. Pharmacol.*, 2020, **113**, 104651.
97 W. Ahmad, M. Zubair, M. Ahmed, M. Ahmad, S. Latif, A. Hameed, *et al.*, Assessment of potentially toxic metal(loid)s contamination in soil near the industrial landfill and impact on human health: an evaluation of risk, *Environ. Geochem. Health*, 2023, **45**(7), 4353–4369.
98 M. A. Karami, Y. Fakhri, S. Rezania, A. A. Alinejad, A. A. Mohammadi, M. Yousefi, *et al.*, Non-Carcinogenic Health Risk Assessment due to Fluoride Exposure from Tea Consumption in Iran Using Monte Carlo Simulation, *Int. J. Environ. Res. Publ. Health*, 2019, **16**, 4261.
99 R. Chen, H. Chen, L. Song, Z. Yao, F. Meng and Y. Teng, Characterization and source apportionment of heavy metals in the sediments of Lake Tai (China) and its surrounding soils, *Sci. Total Environ.*, 2019, **694**, 133819.
100 W. Ma, L. Tai, Z. Qiao, L. Zhong, Z. Wang, K. Fu, *et al.*, Contamination source apportionment and health risk assessment of heavy metals in soil around municipal solid waste incinerator: A case study in North China, *Sci. Total Environ.*, 2018, **631–632**, 348–357.
101 X. Zhang, S. Wei, Q. Sun, S. A. Wadood and B. Guo, Source identification and spatial distribution of arsenic and heavy metals in agricultural soil around Hunan industrial estate by positive matrix factorization model, principle components analysis and geo statistical analysis, *Ecotoxicol. Environ. Saf.*, 2018, **159**, 354–362.
102 A. H. Mahvi, F. Eslami, A. N. Baghani, N. Khanjani, K. Yaghmaeian and H. J. Mansoorian, Heavy metal pollution status in soil for different land activities by contamination indices and ecological risk assessment, *Int. J. Environ. Sci. Technol.*, 2022, **19**(8), 7599–7616.
103 S. Reddy and W. J. Osborne, Heavy metal determination and aquatic toxicity evaluation of textile dyes and effluents using Artemia salina, *Biocatal. Agric. Biotechnol.*, 2020, **25**, 101574.
104 X. Wang, X. Li, X. Yan, C. Tu and Z. Yu, Environmental risks for application of iron and steel slags in soils in China: A review, *Pedosphere*, 2021, **31**(1), 28–42.
105 K. Samrane, M. Latifi, M. Khajouei and A. Bouhaouss, Comprehensive analysis and relevant developments of cadmium removal technologies in fertilizers industry, *Miner. Eng.*, 2023, **201**, 108189.
106 J. A. Adeyemi, J. C. Cruz, T. V. Ayo-Awe, B. A. Rocha, C. O. Adedire, V. C. de Oliveira-Souza, *et al.*, Occurrence of trace elements in print paper products: Non-carcinogenic risk assessment through dermal exposure, *Environ. Res.*, 2023, **237**, 116996.
107 D. M. Bordean, L. Pirvulescu, M. A. Poiana, E. Alexa, A. Cozma, D. N. Raba, *et al.*, An Innovative Approach to Assess the Ecotoxicological Risks of Soil Exposed to Solid Waste, *Sustainability*, 2021, **13**(11), 6141.

108 K. Ashrafi, R. Fallah, M. Hadei, M. Yarahmadi and A. Shahsavani, Source Apportionment of Total Suspended Particles (TSP) by Positive Matrix Factorization (PMF) and Chemical Mass Balance (CMB) Modeling in Ahvaz, Iran, *Arch. Environ. Contam. Toxicol.*, 2018, **75**(2), 278–294.

109 N. Karić, A. S. Maia, A. Teodorović, N. Atanasova, G. Langergraber, G. Crini, *et al.*, Bio-waste valorisation: Agricultural wastes as biosorbents for removal of (in) organic pollutants in wastewater treatment, *Chem. Eng. J. Adv.*, 2022, **9**, 100239.

110 P. Sivaperumal, T. Sankar and P. Viswanathannair, Heavy metal concentrations in fish, shellfish and fish products from internal markets of India vis-a-vis international standards, *Food Chem.*, 2007, **102**(3), 612–620.

111 K. Pivnenko, E. Eriksson and T. F. Astrup, Waste paper for recycling: Overview and identification of potentially critical substances, *Waste Manage.*, 2015, **45**, 134–142.

112 G. M. Elmas and G. Çınar, Toxic Metals in Paper and Paperboard Food Packagings, *Bioresources*, 2018, **13**(4), 7560–7580.

113 A. Turner, Heavy Metals in the Glass and Enamels of Consumer Container Bottles, *Environ. Sci. Technol.*, 2019, **53**(14), 8398–8404.

114 D. Pant and P. Singh, Pollution due to hazardous glass waste, *Environ. Sci. Pollut. Res.*, 2014, **21**(4), 2414–2436.

115 X. Zeng, D. Liu, Y. Wu, L. Zhang, R. Chen, R. Li, *et al.*, Heavy metal risk of disposable food containers on human health, *Ecotoxicol. Environ. Saf.*, 2023, **255**, 114797.

116 S. A. Viczek, A. Aldrian, R. Pomberger and R. Sarc, Origins and carriers of Sb, As, Cd, Cl, Cr, Co, Pb, Hg, and Ni in mixed solid waste – A literature-based evaluation, *Waste Manage.*, 2020, **103**, 87–112.

117 S. Qu, Q. Shi, G. Zhang, X. Dong and X. Xu, Effects of soldering temperature and preheating temperature on the properties of Sn–Zn solder alloys using wave soldering, *Solder. Surf. Mt. Technol.*, 2024, 108–116.

118 M. P. Cenci, D. D. Munchen, J. C. Mengue Model and H. M. Veit, Metal Resources in Electronics: Trends, Opportunities and Challenges, in *Management of Electronic Waste*, Wiley, 2024, pp. 114–151, DOI: 10.1002/9781119894360.ch6.

119 M. Radetić and D. Marković, Nano-finishing of cellulose textile materials with copper and copper oxide nanoparticles, *Cellulose*, 2019, **26**(17), 8971–8991.

120 M. Herrero, J. Rovira, M. Nadal and J. L. Domingo, Risk assessment due to dermal exposure of trace elements and indigo dye in jeans: Migration to artificial sweat, *Environ. Res.*, 2019, **172**, 310–318.

121 M. F. Sima, Determination of some heavy metals and their health risk in T-shirts printed for a special program, *PLoS One*, 2022, **17**(9), e0274952.

122 S. Bolan, A. Kunhikrishnan, B. Seshadri, G. Choppala, R. Naidu, N. S. Bolan, *et al.*, Sources, distribution, bioavailability, toxicity, and risk assessment of heavy metal(loid)s in complementary medicines, *Environ. Int.*, 2017, **108**, 103–118.

123 M. Adnan, B. Xiao, P. Xiao, P. Zhao and S. Bibi, Heavy Metal, Waste, COVID-19, and Rapid Industrialization in This Modern Era—Fit for Sustainable Future, *Sustainability*, 2022, **14**(8), 4746.

124 W. Shen, N. Zhu, Y. Xi, J. Huang, F. Li, P. Wu, *et al.*, Effects of medical waste incineration fly ash on the promotion of heavy metal chlorination volatilization from incineration residues, *J. Hazard. Mater.*, 2022, **425**, 128037.

125 J. K. McIntyre, N. Winters, L. Rozmyn, T. Haskins and J. D. Stark, Metals leaching from common residential and commercial roofing materials across four years of weathering and implications for environmental loading, *Environ. Pollut.*, 2019, **255**, 113262.

126 D. O'Connor, D. Hou, J. Ye, Y. Zhang, Y. S. Ok, Y. Song, *et al.*, Lead-based paint remains a major public health concern: A critical review of global production, trade, use, exposure, health risk, and implications, *Environ. Int.*, 2018, **121**, 85–101.

127 P. J. Harvey, H. K. Handley and M. P. Taylor, Widespread copper and lead contamination of household drinking water, New South Wales, Australia, *Environ. Res.*, 2016, **151**, 275–285.

128 J. E. Emurotu, E. C. Azike, O. M. Emurotu and Y. A. Umar, Chemical fractionation and mobility of Cd, Mn, Ni, and Pb in farmland soils near a ceramics company, *Environ. Geochem. Health*, 2024, **46**(7), 241.

129 H. Jeong, J. S. Ryu and K. Ra, Characteristics of potentially toxic elements and multi-isotope signatures (Cu, Zn, Pb) in non-exhaust traffic emission sources, *Environ. Pollut.*, 2022, **292**, 118339.

130 S. Singh and N. L. Devi, Heavy Metal Pollution in Atmosphere from Vehicular Emission, in *Heavy Metal Toxicity: Environmental Concerns, Remediation and Opportunities*, Springer Nature Singapore, Singapore, 2023, pp. 183–207.

131 D. Lacerda, I. A. Pestana, C. dos Santos Vergilio and C. E. de Rezende, Global decrease in blood lead concentrations due to the removal of leaded gasoline, *Chemosphere*, 2023, **324**, 138207.

132 M. Kaya, Galvanizing residue and electrical Arc Furnace (EAF) dust, *Recycling Technologies for Secondary Zn-Pb Resources*, Springer International Publishing, Cham, 2023, pp. 71–150, DOI: 10.1007/978-3-031-14685-5_4.

133 S. Selonen, A. Dolar, A. Jemec Kokalj, L. N. A. Sackey, T. Skalar, V. Cruz Fernandes, *et al.*, Exploring the impacts of microplastics and associated chemicals in the terrestrial environment – Exposure of soil invertebrates to tire particles, *Environ. Res.*, 2021, **201**, 111495.

134 K. C. Ajah, J. Ademiluyi and C. C. Nnaji, Spatiality, seasonality and ecological risks of heavy metals in the vicinity of a degenerate municipal central dumpsite in Enugu, Nigeria, *J. Environ. Health Sci. Eng.*, 2015, **13**(1), 15.

135 Y. Hu, X. Liu, J. Bai, K. Shih, E. Y. Zeng and H. Cheng, Assessing heavy metal pollution in the surface soils of a region that had undergone three decades of intense industrialization and urbanization, *Environ. Sci. Pollut. Res.*, 2013, **20**(9), 6150–6159.

136 A. Kabata-Pendias, *Trace Elements in Soils and Plants*, CRC Press, London, 4th edn, 2010.
137 T. Jin, J. Lu and M. Nordberg, Toxicokinetics and biochemistry of cadmium with special emphasis on the role of metallothionein, *Neurotoxicology*, 1998, **19**(4–5), 529–535.
138 K. Weggler, M. J. McLaughlin and R. D. Graham, Effect of Chloride in Soil Solution on the Plant Availability of Biosolid-Borne Cadmium, *J. Environ. Qual.*, 2004, **33**(2), 496–504.
139 A. Dutta, A. Patra, H. Singh Jatav, S. Singh Jatav, S. Kumar Singh, E. Sathyanarayana, *et al.*, Toxicity of Cadmium in Soil-Plant-Human Continuum and Its Bioremediation Techniques, in *Soil Contamination – Threats and Sustainable Solutions*, IntechOpen, 2021.
140 R. Bagheri, H. Bashir, J. Ahmad, A. Baig and M. I. Qureshi, Efects of cadmium stress on plants, *Environ. Sustainability*, 2014, 271–277.
141 H. S. Kim, B. H. Seo, G. Owens, Y. N. Kim, J. H. Lee, M. Lee, *et al.*, Phytoavailability-based threshold values for cadmium in soil for safer crop production, *Ecotoxicol. Environ. Saf.*, 2020, **201**, 110866.
142 M. Zubair, P. M. Adnan Ramzani, B. Rasool, M. A. Khan, M. Ur-Rahman, I. Akhtar, *et al.*, Efficacy of chitosan-coated textile waste biochar applied to Cd-polluted soil for reducing Cd mobility in soil and its distribution in moringa (Moringa oleifera L.), *J. Environ. Manage.*, 2021, **284**, 112047.
143 P. Jali, C. Pradhan and A. B. Das, Effects of Cadmium Toxicity in Plants: A Review Article, *J. Biosci.*, 2016, **4**(12), 1074–1081.
144 A. Zaid, J. A. Bhat, S. H. Wani and K. Z. Masoodi, Role of Nitrogen and Sulfur in Mitigating Cadmium induced Metabolism Alterations in Plants, *J. Plant Sci. Res.*, 2019, **35**(1), 121–141.
145 N. Baruah, N. Gogoi, S. Roy, P. Bora, J. Chetia, N. Zahra, *et al.*, Phytotoxic Responses and Plant Tolerance Mechanisms to Cadmium Toxicity, *J. Soil Sci. Plant Nutr.*, 2023, **23**(4), 4805–4826.
146 F. U. Haider, C. Liqun, J. A. Coulter, S. A. Cheema, J. Wu, R. Zhang, *et al.*, Cadmium toxicity in plants: Impacts and remediation strategies, *Ecotoxicol. Environ. Saf.*, 2021, **211**, 111887.
147 V. Unsal, T. Dalkiran, M. Çiçek and E. Kölükçü, The Role of Natural Antioxidants Against Reactive Oxygen Species Produced by Cadmium Toxicity: A Review, *Adv. Pharm. Bull.*, 2020, **10**(2), 184–202.
148 T. Abbas, M. Rizwan, S. Ali, M. Adrees, M. Zia-ur-Rehman, M. F. Qayyum, *et al.*, Effect of biochar on alleviation of cadmium toxicity in wheat (Triticum aestivum L.) grown on Cd-contaminated saline soil, *Environ. Sci. Pollut. Res.*, 2018, **25**(26), 25668–25680.
149 R. Shen, K. Hussain, N. Liu, J. Li, J. Yu, J. Zhao, *et al.*, Ecotoxicity of Cadmium along the Soil-Cotton Plant-Cotton Bollworm System: Biotransfer, Trophic Accumulation, Plant Growth, Induction of Insect Detoxification Enzymes, and Immunocompetence, *J. Agric. Food Chem.*, 2024, **72**(25), 14326–14336.
150 G. Genchi, M. S. Sinicropi, G. Lauria, A. Carocci and A. Catalano, The Effects of Cadmium Toxicity, *Int. J. Environ. Res. Publ. Health*, 2020, **17**(11), 3782.
151 Z. Jia, S. Li and L. Wang, Assessment of soil heavy metals for eco-environment and human health in a rapidly urbanization area of the upper Yangtze Basin, *Sci. Rep.*, 2018, **8**(1), 3256.
152 B. Hu, X. Jia, J. Hu, D. Xu, F. Xia and Y. Li, Assessment of Heavy Metal Pollution and Health Risks in the Soil-Plant-Human System in the Yangtze River Delta, China, *Int. J. Environ. Res. Publ. Health*, 2017, **14**(9), 1042.
153 Y. Jin, D. O'Connor, Y. S. Ok, D. C. W. Tsang, A. Liu and D. Hou, Assessment of sources of heavy metals in soil and dust at children's playgrounds in Beijing using GIS and multivariate statistical analysis, *Environ. Int.*, 2019, **124**, 320–328.
154 V. Kumar, S. Pandita, A. Sharma, P. Bakshi, P. Sharma, I. Karaouzas, *et al.*, Ecological and human health risks appraisal of metal(loid)s in agricultural soils: a review, *Geol. Ecol. Landsc.*, 2021, **5**(3), 173–185.
155 WHO, *Children and Digital Dumpsites: E-Waste Exposure and Child Health*, 2021.
156 Y. Gong, Y. Wu, C. Lin, D. Xu, X. Duan, B. Wang, *et al.*, Is hand-to-mouth contact the main pathway of children's soil and dust intake?, *Environ. Geochem. Health*, 2022, **44**(5), 1567–1580.
157 A. M. Wilson, M. P. Verhougstraete, P. I. Beamer, M. F. King, K. A. Reynolds and C. P. Gerba, Frequency of hand-to-head, -mouth, -eyes, and -nose contacts for adults and children during eating and non-eating macro-activities, *J. Expo. Sci. Environ. Epidemiol.*, 2021, **31**(1), 34–44.
158 L. T. Ogundele, O. K. Owoade, P. K. Hopke and F. S. Olise, Heavy metals in industrially emitted particulate matter in Ile-Ife, Nigeria, *Environ. Res.*, 2017, **156**, 320–325.
159 O. Olujimi, O. Steiner and W. Goessler, Pollution indexing and health risk assessments of trace elements in indoor dusts from classrooms, living rooms and offices in Ogun State, Nigeria, *J. Afr. Earth Sci.*, 2015, **101**, 396–404.
160 A. Miletić, M. Lučić and A. Onjia, Exposure Factors in Health Risk Assessment of Heavy Metal(loid)s in Soil and Sediment, *Metals*, 2023, **13**(7), 1266.
161 J. F. Gonçalves, V. L. Dressler, C. E. Assmann, V. M. M. Morsch and M. R. C. Schetinger, Cadmium neurotoxicity: From its analytical aspects to neuronal impairment, in *Advances in Neurotoxicology*, ed. M. Aschner and L. G. Costa, Academic Press, 2021, vol. 5, pp. 81–113, DOI: **10.1016/bs.ant.2021.03.001**.
162 Y. G. Gu, Q. Lin and Y. P. Gao, Metals in exposed-lawn soils from 18 urban parks and its human health implications in southern China's largest city, Guangzhou, *J. Clean. Prod.*, 2016, **115**, 122–129.
163 M. Kippler, F. Tofail, J. D. Hamadani, R. M. Gardner, S. M. Grantham-McGregor, M. Bottai, *et al.*, Early-Life Cadmium Exposure and Child Development in 5-Year-Old

Girls and Boys: A Cohort Study in Rural Bangladesh, *Environ. Health Perspect.*, 2012, **120**(10), 1462–1468.

164 K. Gustin, F. Tofail, M. Vahter and M. Kippler, Cadmium exposure and cognitive abilities and behavior at 10 years of age: A prospective cohort study, *Environ. Int.*, 2018, **113**, 259–268.

165 M. Radfard, H. Hashemi, M. A. Baghapour, M. R. Samaei, M. Yunesian, H. Soleimani, *et al.*, Prediction of human health risk and disability-adjusted life years induced by heavy metals exposure through drinking water in Fars Province, Iran, *Sci. Rep.*, 2023, **13**(1), 19080.

166 N. M. Smereczański and M. M. Brzóska, Current Levels of Environmental Exposure to Cadmium in Industrialized Countries as a Risk Factor for Kidney Damage in the General Population: A Comprehensive Review of Available Data, *Int. J. Mol. Sci.*, 2023, **24**(9), 8413.

167 A. Piperno, S. Pelucchi and R. Mariani, Inherited iron overload disorders, *Transl. Gastroenterol. Hepatol.*, 2020, **5**, 25.

168 G. J. Anderson and E. Bardou-Jacquet, Revisiting hemochromatosis: genetic vs. phenotypic manifestations, *Ann. Transl. Med.*, 2021, **9**(8), 731.

169 L. Mezzaroba, D. F. Alfieri, A. N. Colado Simão and E. M. Vissoci Reiche, The role of zinc, copper, manganese and iron in neurodegenerative diseases, *Neurotoxicology*, 2019, **74**, 230–241.

170 B. Nemery, Metals and the respiratory tract, in *Handbook on the Toxicology of Metals*, Elsevier, 2022, pp. 421–443.

171 O. K. Kurt and N. Basaran, Occupational Exposure to Metals and Solvents: Allergy and Airway Diseases, *Curr. Allergy Asthma Rep.*, 2020, **20**(8), 38.

172 S. Bello, R. Nasiru, N. N. Garba and D. J. Adeyemo, Carcinogenic and non-carcinogenic health risk assessment of heavy metals exposure from Shanono and Bagwai artisanal gold mines, Kano state, Nigeria, *Sci. Afr.*, 2019, **6**, e00197.

173 H. Guo, H. Liu, H. Wu, H. Cui, J. Fang, Z. Zuo, *et al.*, Nickel Carcinogenesis Mechanism: DNA Damage, *Int. J. Mol. Sci.*, 2019, **20**(19), 4690.

174 N. B. Silverberg, J. L. Pelletier, S. E. Jacob, L. C. Schneider, B. Cohen, K. A. Horii, C. L. Kristal, S. M. Maguiness, M. M. Tollefson, M. G. Weinstein, T. S. Wright, A. C. Yan, E. C. Matsui, J. A. Bird, C. M. Davis, V. P. Hernandez-Trujillo, J. S. Orange, M. Pistiner and J. Wang, Nickel Allergic Contact Dermatitis: Identification, Treatment, and Prevention, *Pediatrics*, 2020, **145**(5), e20200628.

175 J. C. Ho, H. J. Wen, C. W. Sun, S. F. Tsai, P. H. Su, C. L. Chang, *et al.*, Prenatal exposure to nickel and atopic dermatitis at age 3 years: a birth cohort study with cytokine profiles, *J. Eur. Acad. Dermatol. Venereol.*, 2022, **36**(12), 2414–2422.

176 Y. Peng, J. Hu, Y. Li, B. Zhang, W. Liu, H. Li, *et al.*, Exposure to chromium during pregnancy and longitudinally assessed fetal growth: Findings from a prospective cohort, *Environ. Int.*, 2018, **121**, 375–382.

177 S. K. Banu, J. A. Stanley, R. J. Taylor, K. K. Sivakumar, J. A. Arosh, L. Zeng, *et al.*, Sexually Dimorphic Impact of Chromium Accumulation on Human Placental Oxidative Stress and Apoptosis, *Toxicol. Sci.*, 2018, **161**(2), 375–387.

178 P. Mitra, S. Sharma, P. Purohit and P. Sharma, Clinical and molecular aspects of lead toxicity: An update, *Crit. Rev. Clin. Lab Sci.*, 2017, **54**(7–8), 506–528.

179 Y. Liu, X. Huo, L. Xu, X. Wei, W. Wu, X. Wu, *et al.*, Hearing loss in children with e-waste lead and cadmium exposure, *Sci. Total Environ.*, 2018, **624**, 621–627.

180 P. Xu, Z. Chen, Y. Chen, L. Feng, L. Wu, D. Xu, *et al.*, Body burdens of heavy metals associated with epigenetic damage in children living in the vicinity of a municipal waste incinerator, *Chemosphere*, 2019, **229**, 160–168.

181 J. G. Dórea, Environmental exposure to low-level lead (Pb) co-occurring with other neurotoxicants in early life and neurodevelopment of children, *Environ. Res.*, 2019, **177**, 108641.

182 FME, Types of solid waste in Uyo metropolis, *A Report of the Federal Ministry of Environment Uyo*, Nigeria, 2013.

183 G. A. Idowu, Heavy metals research in Nigeria: a review of studies and prioritization of research needs, *Environ. Sci. Pollut. Res.*, 2022, **29**(44), 65940–65961.

184 C. Du and Z. Li, Contamination and health risks of heavy metals in the soil of a historical landfill in northern China, *Chemosphere*, 2023, **313**, 137349.

185 J. He, C. Li, X. Tan, Z. Peng, H. Li, X. Luo, *et al.*, Driving factors for distribution and transformation of heavy metals speciation in a zinc smelting site, *J. Hazard. Mater.*, 2024, **471**, 134413.

186 L. Liu, W. Ouyang, Y. Wang, M. Tysklind, F. Hao, H. Liu, *et al.*, Heavy metal accumulation, geochemical fractions, and loadings in two agricultural watersheds with distinct climate conditions, *J. Hazard. Mater.*, 2020, **389**, 122125.